Transportation Research Part D 133 (2024) 104164

Contents lists available at ScienceDirect

Transportation Research Part D

journal homepage: www.elsevier.com/locate/trd

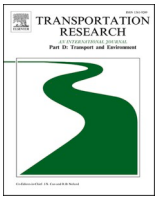

Sources of subway $PM_{2.5}$: Investigation of a system with limited mechanical ventilation

Keith Van Ryswyk [a,b,*], Ryan Kulka [a], Cheol-Heon Jeong [b], Angelos T. Anastasopolos [a], Tim Shin [a], Peter Blanchard [c], Danielle Veikle [c], Greg J. Evans [b]

[a] Air Pollution Exposure Science Section, Water and Air Quality Bureau, Health Canada, Ottawa, Ontario, Canada
[b] Department of Chemical Engineering and Applied Chemistry, University of Toronto, Toronto, Ontario, Canada
[c] Canadian Light Source, Saskatoon, Saskatchewan, Canada

ARTICLE INFO

Keywords:
Subway
Air quality
Source apportionment
Particulate matter
Piston effect
Ventilation

ABSTRACT

Identifying subway PM sources is essential to improving subway air quality. To date, no source apportionment studies exist for systems with limited mechanical ventilation. These systems often have high concentrations of $PM_{2.5}$. This study investigated $PM_{2.5}$ sources in the Toronto subway system using three analytical approaches. Positive matrix factorization identified three subway sources and no outdoor sources. A two-source Chemical Mass Balance (CMB) model apportioned 92% and 55% of $PM_{2.5}$ to iron-rich components (wheels, rails, and contact rails & shoes) and 8% and 45% to brake pads on line 1 and 2, respectively. A simple mechanistic model combined with the CMB results revealed wear of wheels, rails, and brake pads during braking to be the main source of $PM_{2.5}$ in this subway. These results indicate that below grade subways with minimal mechanical ventilation are dominated by system-sourced $PM_{2.5}$ emitted during deceleration. This knowledge should help identify strategies to improve air quality in the subway systems.

1. Introduction

Particulate air pollution in subways is an ongoing public health concern. While questions remain regarding the health effects of these uniquely iron-rich particles (Loxham and Nieuwenhuijsen, 2019), the high mass concentration of fine particulate matter (PM) less than 2.5 μm in aerodynamic diameter ($PM_{2.5}$) in subway environments alone has resulted in calls for its mitigation (COMEAP, 2019; TPH, 2020). Moreover, air quality standards specific to subway platforms are being introduced. The Korean Indoor Air Quality Management Act includes critical values of 50 $\mu g/m^3$ for $PM_{2.5}$ and 100 $\mu g/m^3$ for PM_{10} (KMOE, 2005; KMOE, 2020). Taiwan's indoor air quality legislation sets maximum levels of 35 $\mu g/m^3$ for $PM_{2.5}$ and 75 $\mu g/m^3$ for PM_{10} (TIAQMA, 2011). Achieving these standards would present a challenge for many systems. A review of published $PM_{2.5}$ concentrations for 115 platforms ranged from 16 to 480 $\mu g/m^3$ (Moreno and de Miguel, 2018). Reductions in the range of an order of magnitude would be required for subway lines that are mostly below grade and have limited use of existing mechanical ventilation systems. Such lines feature the highest PM concentrations reported in the subway air quality literature and comprise an extensive proportion of the systems of London (Saunders et al., 2019), Shanghai (Zhao et al., 2017), Copenhagen (Kappelt et al., 2022), the northeastern United States (Luglio et al., 2021; Azad et al., 2023)

* Corresponding author at: 269 Laurier Ave West, Ottawa, Ontario K1A 0K9, Canada.
E-mail address: Keith.VanRyswyk@hc-sc.gc.ca (K. Van Ryswyk).

https://doi.org/10.1016/j.trd.2024.104164
Received 5 July 2023; Received in revised form 12 March 2024; Accepted 12 March 2024
Available online 29 June 2024

and Toronto (Van Ryswyk et al., 2021). In most countries, the existence of station and tunnel mechanical ventilation systems are mandated by federal safety regulations. They also maintain thermal thresholds, activating when they are exceeded. Systems such as those of Montreal and Barcelona require continuous mechanical ventilation for cooling and, as a result, have relatively lower PM concentrations and significant seasonality with lower PM in summer when more ventilation is required to manage heat (Martins et al., 2015, Moreno et al., 2017b, Van Ryswyk et al., 2017). For some subways lines, the piston effect is sufficient to maintain thermal comfort levels and the existing mechanical ventilation systems have limited use. The resulting higher PM concentrations of these lines suggest that the ability of the piston effect to remove PM from the system is limited relative to mechanical ventilation. Stations of the Barcelona system with narrow platforms were observed to have significantly higher PM concentrations when forced tunnel ventilaton was turned off (Moreno et al., 2014). There is evidence of its impact on PM via tunnel openings. For the systems of Vancouver and Toronto, $PM_{2.5}$ concentrations were 6.3% and 8.6% lower per km of proximity to tunnel openings, respectively (Van Ryswyk et al., 2017). This same relationship was observed in the Copenhagen system but limited to within 3 km of tunnel openings (Kappelt et al., 2022). Further, Copenhagen's newly opened M3 line, a completely below grade closed loop, featured the highest PM concentrations in the entire system (168 $\mu g/m^3$). Overall, this suggests the PM reducing potential of the piston effect to be far lower than mechanical ventilation and limited to sections in close proximity to tunnel openings.

A wide variety of approaches have been explored to improve subway air quality (Park et al., 2019). Many of these involve increasing the rate of PM removal from subway environments through filtration or increasing ventilation. To meet the $PM_{2.5}$ and PM_{10} standards in the Seoul Metropolitan Subway, automated ventilation protocols were developed (Kim et al., 2016b,a; Lee et al., 2015; Liu et al., 2013; Loy-Benitez et al., 2018, 2021). However, system design changes to increase ventilation efficiency or continual operation of ventilation systems can be costly. To constrain energy costs, inputs such as outdoor PM levels, time of day, and train schedules are used to ensure that the use of ventilation does not go beyond what is needed to maintain standards. Platform PM concentrations are a critical input for these systems. Therefore, reducing the rate of subway-sourced PM emission may also be an effective approach to decreasing the costs of ventilation and other PM removal methods such as filtration. Indeed, the combination of decreasing the rate of PM generation and increasing the rate of its removal may constitute the ideal two-pronged approach to sustainable and effective subway air quality management.

The potential to reduce subway-sourced PM emission is significant considering the high proportion of subway PM that can originate from within the system. This is evidenced by a common finding that subway PM contains a high proportion of iron, which is the major elemental constituent of subway components such as wheels, running and contact rails, brake lining material (brake pads), and current-carrying materials such as contact shoes or catenaries and pantographs (Bachoual et al., 2007; Cusack et al., 2015; Font et al., 2019; Lee et al., 2018; Loxham et al., 2013; Luglio et al., 2021; Minguillón et al., 2018; Moreno et al., 2015; Park et al., 2014a; Querol et al., 2012; Smith et al., 2020; Van Ryswyk et al., 2021). The abundance of other elements and their ratio to Fe often reflect the composition of steel (Chillrud et al., 2004; Moreno et al., 2015; Van Ryswyk et al., 2017). Finally, analyses of subway particle morphology and composition have described the high-temperature frictional forces and subsequent oxidation which create the ferruginous amorphous particle type that dominates the mass concentrations of subway PM (Moreno et al., 2015, 2017a). Apportioning the 'subway source' between subway system components (e.g., wheel/rail wear emissions, brake wear emissions, current-carrying material emissions, etc.) can potentially inform strategies to reduce the rate of system-sourced PM emission. Various studies have attempted to apportion subway PM to single subway components. To date, five studies have identified subway PM sources and the estimated their contribution to total subway PM. Each of these studies employed positive matrix factorization (PMF) analyses using chemical speciation data to identify and apportion sources. Samples were analysed for major and trace elements, water-soluble ions and carbon. Information on the oxide species of elements has also been generated. These studies were conducted in the Seoul Metropolitan Subway (Park et al., 2014a; Park et al., 2012), the Nanchang metro (Huang et al., 2021), and the Barcelona Subway System (Martins et al., 2016; Minguillón et al., 2018). The two Seoul studies indicated that 48% (Park et al., 2012) and 68% (Park et al., 2014a) of PM_{10} was sourced from subway components. The Nanchang study identified three non-subway sources (coal combustion, vehicle exhaust, and industrial) from infiltrated outdoor ambient air to contribute 53% of $PM_{2.5}$ while the subway system component 'wheel/rail' and 'brake and pantograph' sources contributed 25% and 4%, respectively. The high contribution of outdoor sources to the subway microenvironment was consistent with the similar concentrations of $PM_{2.5}$ between trains (179 ± 48 $\mu g/m^3$) and platforms (122 ± 22 $\mu g/m^3$) and the outdoors (176 ± 30 $\mu g/m^3$). The first of the Barcelona studies (Martins et al., 2016) collected $PM_{2.5}$ samples in the cold and warm seasons and stratified its PMF analysis by two seasons and four stations. This analytical approach revealed the impact of ventilation on the contribution of the subway to its own $PM_{2.5}$. In Barcelona's system, continuous ventilation is used to maintain thermal comfort for passengers, which is less intense in the colder season. The contribution of the system itself to the $PM_{2.5}$ of these four stations ranged from 17 to 46% in the warmer season and 50–85% in the colder season. The samples of these four stations were combined with those of a second sampling campaign for a 406-sample PMF analysis of the $PM_{2.5}$ (Minguillón et al., 2018). In this analysis, 11 stations of 7 lines were represented in the data. No stratification of the PMF analysis was conducted and ten sources were identified. Five factors represented line-specific subway component sources: a combined rail and wheel factor, two brake factors, a lead-rich factor, and a mixed factor representing combined rail/wheels/brake emissions. As with the previous study of the Barcelona system, increased ventilation during the warm season decreased the contribution of subway sources to the total $PM_{2.5}$. The impact of subway platform design was evident as well. Subway component sources contributed to 43–91% of $PM_{2.5}$ in the older stations and 21–52% in the newer stations. The new stations featured full platform screen doors which inhibit the movement of air between the tracks (where friction-generated PM emission and PM-resuspension take place) and the subway platforms and other passenger areas (Moreno et al., 2015, 2017b, Park et al., 2014a,b). This study, with its high number of samples representing several stations and lines and line-specific information on the chemical composition of subway components, was able to separate the 'subway source' into its various components. For example, a brake-specific factor contributed 15–35% of $PM_{2.5}$ on lines 1 and 3, 36–52% on line 4, and 4–14%

on lines 2 and 10. Overall, brakes contributed more than other subway component, which the authors then concluded should be the target for reducing subway-sourced PM emissions. Overall, this body of research exemplifies the impact of ventilation and subway component material on the variability of subway-sourced PM.

The Subway Air Quality Initiative aimed to estimate the proportion of subway $PM_{2.5}$ that originates from within a subway system itself and from individual subway components. This information can inform approaches on mitigating subway-sourced PM and reduce overall $PM_{2.5}$ concentrations. Several approaches were employed to identify $PM_{2.5}$ sources and estimate their contributions to total $PM_{2.5}$. PMF receptor modelling was used to resolve factors from sampled $PM_{2.5}$ elemental composition data and related these to subway component sources. A Chemical Mass Balance (CMB) receptor model was also employed to apportion $PM_{2.5}$ to sources. Finally, a mechanistic approach to subway source apportionment was explored. This work represents the first study investigating $PM_{2.5}$ sources within a subway system using limited mechanical ventilation.

2. Methods

The Subway Air Quality Initiative research study sampled $PM_{2.5}$ and coarse PM ($PM_{2.5\text{-}10}$) on 22 platforms of a subway system in Toronto, Canada from December 2017 – August 2018. An analysis of the $PM_{2.5}$ data investigated the impact of system changes on subway air quality and is published elsewhere (Van Ryswyk et al., 2021). This manuscript presents the mass concentrations of the integrated $PM_{2.5}$ and $PM_{2.5\text{-}10}$ samples collected in the study as well as several analyses on the physiochemical properties and sources of the $PM_{2.5}$ samples.

2.1. PM sample collection

Samples of $PM_{2.5}$ and $PM_{2.5\text{-}10}$ were collected for 12-h (6:00 am to 6:00 pm) in 11 underground stations from each of the Toronto subway's two main lines: Line 1 (a.k.a. the 'Yonge-University line') and line 2 (a.k.a. the 'Bloor-Danforth line'); reference samples were also collected at two nearby outdoor sites. Stations were selected based on the projected scheduling of a track bed vacuum car. When it

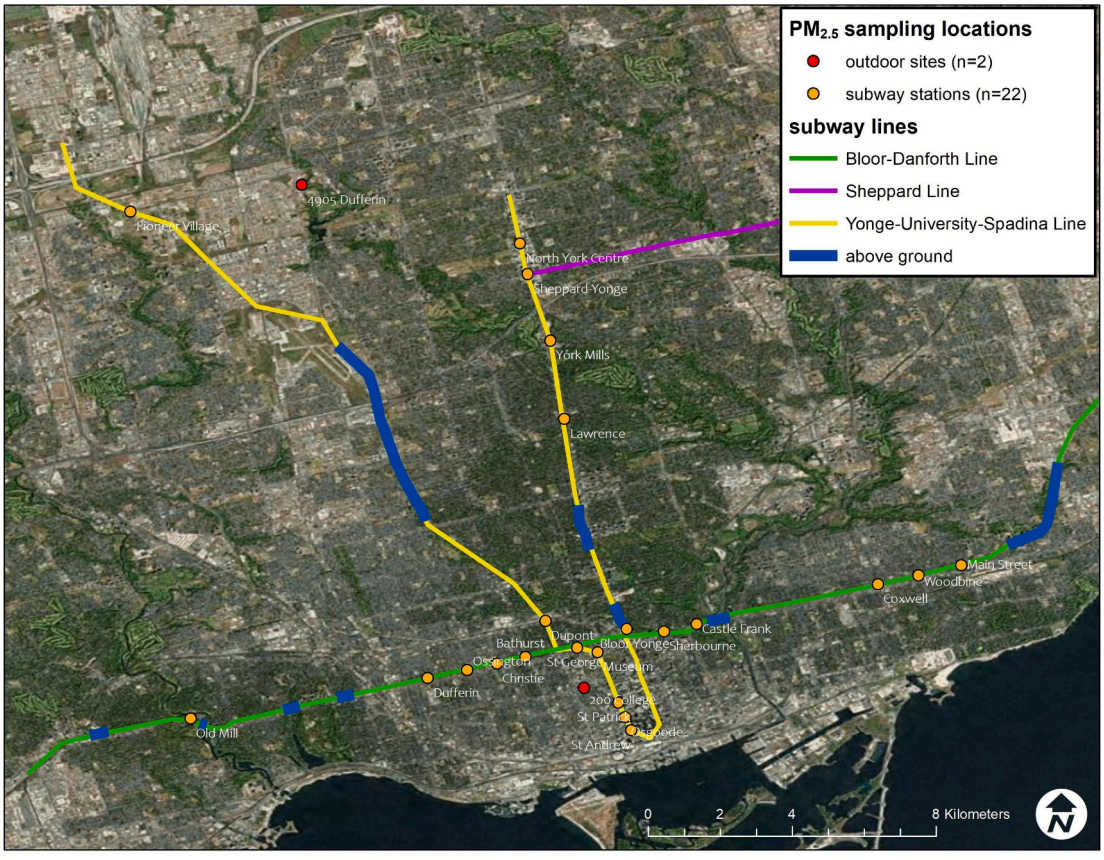

Fig. 1. Subway and outdoor air sampling locations.

was not in use, stations were selected to broaden the representation of stations across the two lines (line 1 and line 2). Sampling was conducted at the end of each platform where trains enter the station. The two outdoor sites were selected to be representative of outdoor $PM_{2.5}$ and $PM_{2.5\text{-}10}$ in Toronto and these samples were collected concurrently with the subway campaign. The locations of the subway platforms and outdoor sites are presented in Fig. 1.

PM sampling used Harvard School of Public Health's Cascade Impactors (CI) and programmable pumps at a flow rate of 5 lpm. $PM_{2.5}$ and $PM_{2.5\text{-}10}$ were captured on 37 mm Teflon filter and polyurethane foam (PUF) media, respectively. Samples ran for 12-hours from 6AM-6PM time periods, daily, on subway platforms. Outdoor samples of $PM_{2.5}$ and $PM_{2.5\text{-}10}$ were collected for one week. Filters were preconditioned for 24 hr before gravimetric analysis. Field technicians ensured sample flows were within 10% of target flows before and after sampling. Field blanks were deployed for every 10 samples for blank correction. If elemental concentrations were above detection in $>$ 50% of blanks, the median blank value was used to blank-correct samples.

2.2. Physiochemical characterization of $PM_{2.5}$: XRF, SEM, & XANES analyses

The elemental content of $PM_{2.5}$ was determined via X-ray fluorescence (XRF) according to United States Environmental Protection Agency (EPA) Method IO-3.3 in Compendium of Methods for the Determination of Metals in Ambient Particulate Matter. The suite of elements analysed included Ag, Al, As, Ba, Br, Ca, Cd, Ce, Cl, Co, Cr, Cs, Cu, Fe, In, K, Mg, Mn, Na, Ni, P, Pb, Rb, S, Sb, Se, Si, Sn, Sr, Ti, V, Zn, and Zr. Electron microscope analysis was carried out using a Thermo Scientific Quattro Environmental Scanning Electron Microscope (ESEM) at an accelerating voltage of 15 keV and a pressure of 50 Pa. A single $PM_{2.5}$ sample from line 1 and line 2 was mounted onto the sample holder with carbon tape to maintain electrical contact between the sample and the stage. Backscattered and secondary electron images were collected at various magnifications. K-edge X-ray absorption near-edge structure (XANES) spectroscopy was used to characterize various oxide, hydroxide and sulfide species of Fe, Cr, Cu, Mn, Ni, and Zn. These elements were chosen on account of their abundance (Fe) and heterogeneity in toxicity across potential species. XANES spectra were collected from the IDEAS (08B2-1) bending magnet beamline at the Canadian Light Source (CLS). The K-edge absorption energy of the reference foils used for energy calibration, as well as the standard compounds used to analyze the XANES data are presented in Table S1. Samples were collected in fluorescence mode with a reference foil collected in transmission mode concurrently for calibration. After all spectra were collected and normalized, they were fit to the reference compounds using the Athena software package (Ravel and Newville, 2005) which employs linear combination fitting (LCF) to identify the major species. One to two $PM_{2.5}$ samples from each of the 22 sampled stations were included in the XANES analyses (n = 30 samples).

2.3. Reference material for source profile information

To serve as proxies for emissions profiles, information on the chemical composition was obtained for outdoor $PM_{2.5}$ and subway components including running rails, wheels, conductor rails, contact shoes, wheels, and brake pads (Fig. 2). These sources have accounted for the majority of subway PM in similar studies conducted in Seoul (Park et al., 2014a; Park et al., 2012), Barcelona (Martins et al., 2016; Minguillón et al., 2018) and Nanchang (Huang et al., 2021). Gravel ballast was not included as it is not used in the Toronto subway system. The concurrent outdoor $PM_{2.5}$ samples provided suitable reference data for elemental composition of outdoor $PM_{2.5}$ and comparison with the subway $PM_{2.5}$ composition. Information sheets on the composition/fabrication of the running rails, conductor rails, wheels, and contact shoes were provided by the Toronto Transit Commission (TTC). Component specifications provided maximum percentage by weight for a non-exhaustive set of elements. Information on the composition of conductor rails and contact shoes was also available from a study which used inductively coupled plasma methods to analyse the composition of these main components of a third rail electrification system used in the Stockholm subway system (Cha et al., 2016). For brake pad composition, samples of line 1 and line 2 brake pads were obtained from the TTC and analysed using XRF (Cooper Environmental Service, Xact 625) capable of detecting S, K, Ca, Ti, V, Cr, Mn, Ba, Fe, Co, Ni, Cu, Zn, As, Se, Br, Sr, Pb, Cd, and Sn. While this method was not specific to $PM_{2.5}$ and the analysis method was not the same as that of the subway $PM_{2.5}$ samples, these data generated relative contribution profiles for Ba, Ca, Cr, Cu, Fe, K, Mn, Ni, Pb, S, Si, Sr, Ti, V, As, Co, and Zn in the brake pad material. Using these data, Fe ratios for each element were calculated. Key elemental markers of sources were then identified from the system-specific source profile data (i.e., brake pads, running rails, wheels, contact rails, contact shoes) alongside review of relevant source marker literature.

2.4. Positive Matrix Factorization (PMF) analysis

$PM_{2.5}$-elemental data were used to examine the sources of $PM_{2.5}$ in the Toronto subway system. The United States Environmental Protection Agency (US EPA) Positive Matrix Factorization (PMF) v5.0 (US EPA, 2014) was used to identify and apportion source types to $PM_{2.5}$ mass. The PMF model applies multivariate statistical analysis to trends in a speciated pollutant dataset to yield factors explaining the data variation. Within PMF, resolved factors (F) and relative factor contributions (G) are directly quantified. The chemical profiles of resolved factors can be related to physically meaningful source types based on their species composition and presence of marker elements alongside relevant trends in their factor contributions. Further detail is provided in section 1 of the Supporting Information. Briefly, the PMF method involves the derivation of a solution for a source-receptor mass balance equation which determines the chemical composition and contributions of a specific number of sources. The analysis is based on the correlations of the components within samples (i.e., in this case, the $PM_{2.5}$-elemental compositional data). The elemental species identified in the XRF and XANES analyses were screened for inclusion in the PMF analysis. Species that were above detection in $>$ 80% of the samples with a signal to noise ratio $<$ 0.2 were included in the analysis. Sample uncertainties were derived from the sampling campaign's

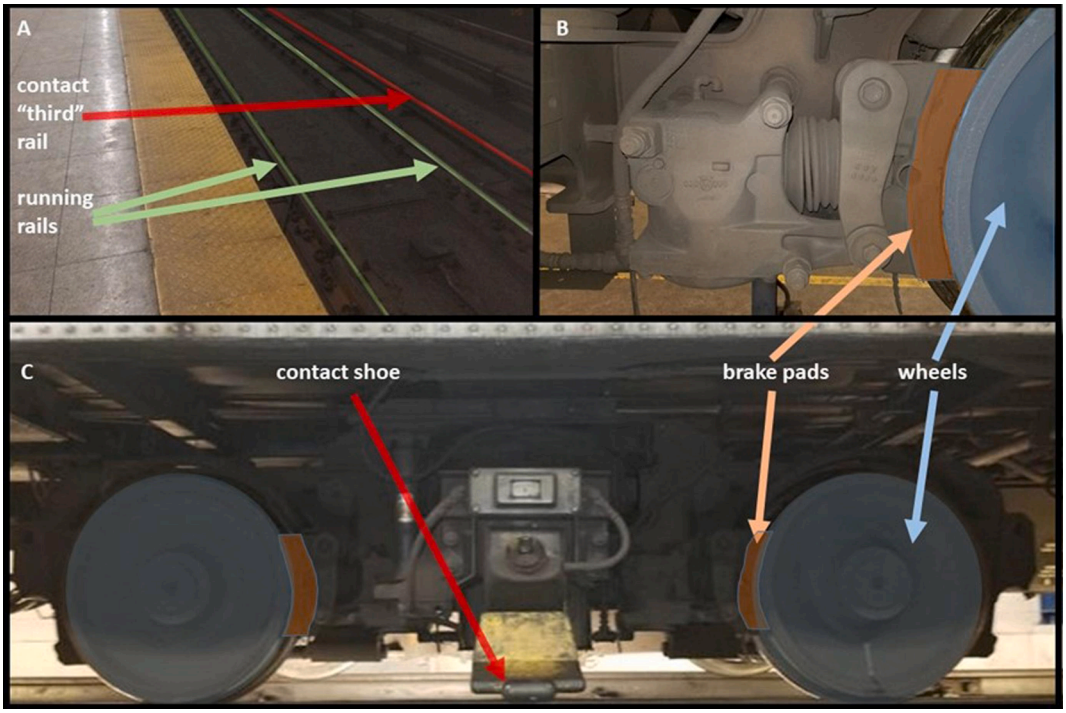

Fig. 2. A: view of track bed from platform with running and contact'third' rails. B: close-up of train bogie with brake and wheel contact. C: full view of train bogie with wheels, brake pads, and contact shoe.

duplicates. Models with two to seven factors were run. The optimal model order retained was selected by balancing good model performance with physically meaningful factors interpretable as source types.

2.5. Chemical mass Balance (CMB) analysis

A CMB model was also used to estimate the contributions of outdoor $PM_{2.5}$ and subway components (brakes, wheels, rails, contact rails, and contact shoes) to subway $PM_{2.5}$. US EPA's CMB 8.0 model (U.S. Environmental Protection Agency, 2004a) was used to estimate source contributions. Source profile information was obtained from the information identified in the compositional analyses of outdoor $PM_{2.5}$ and brake pads as well as from the specifications of subway components (section 2.3). This CMB model applied the variance-weighted least-squares fitting to estimate the contributions of each source to each daily $PM_{2.5}$ sample from the 22 stations included in the study.

3. Results & discussion

The 22 stations included in this study represent locations throughout the two major lines of the Toronto subway system (Fig. 1). They feature a range of station ages, depths, and distances to an above-grade sections (a.k.a 'open cuts'). Information on these design features as well as sampling session dates for the subway and outdoor locations are presented in Table 1. Between 4 and 15 daily samples of $PM_{2.5}$ were collected on each subway platform through one or two multi-day sessions at each station; in total 11 line 1 and 11 line 2 stations were included yielding 201 $PM_{2.5}$ and 224 $PM_{2.5\text{-}10}$ samples. As only 3–5 stations were able to be sampled at a time, each station's data represents one or two of the three seasons (winter, spring or summer) covered during the nine-month campaign. The two outdoor sites were sampled over the course of the spring and summer yielding 23 seven-day samples.

3.1. $PM_{2.5}$ and $PM_{2.5\text{-}10}$ concentrations on platforms

On line 1, average platform $PM_{2.5}$ ranged from 75 $\mu g/m^3$ at Pioneer Village station to 179 $\mu g\ m^{-3}$ at St. George station (Table 1). Line 2 platform $PM_{2.5}$ was significantly higher with station averages ranging from 238 $\mu g\ m^{-3}$ (Ossington) to 497 $\mu g\ m^{-3}$ (Main Street).

Table 1
Monitoring sessions at subway and outdoor sites, station design information, and concentrations of PM2.5 and PM2.5-10.

Subway/ outdoor	station	Opened (year)	Depth (m)	DAG[a] (km)	S #[b]	season	Sampling dates		$PM^{c}_{2.5}$		$PM^{c}_{2.5\text{-}10}$	
							start	end	n	μ (SD)	n	μ (SD)
line 1	dupont	1978	9	3	1	winter	9-Jan-18	14-Jan-18	14	126 (31)	15	123 (24)
					2	winter	7-Feb-18	14-Feb-18				
	lawrence	1973	18	2	1	summer	15-Aug-18	29-Aug-18	6	152 (39)	6	186 (27)
	museum	1963	7	6	1	winter	8-Jan-18	14-Jan-18	15	138 (22)	15	161 (23)
					2	winter	7-Feb-18	14-Feb-18				
	north york centre	1987	13	7	1	summer	21-Aug-18	29-Aug-18	4	126 (36)	4	123 (25)
	osgoode	1963	10	7	1	summer	31-Jul-18	9-Aug-18	4	100 (5)	4	100 (4)
	pioneer village	2017	9	6	1	summer	30-Jul-18	3-Aug-18	5	75 (10)	5	81 (7)
					2	summer	15-Aug-18	17-Aug-18				
	sheppard yonge	1974	4	4	1	summer	16-Aug-18	28-Aug-18	5	104 (19)	5	114 (16)
	st. andrew	1963	12	8	1	summer	30-Jul-18	10-Aug-18	5	99 (17)	5	127 (14)
	st. george	1963	10	5	1	winter	8-Jan-18	14-Jan-18	15	179 (61)	15	169 (43)
					2	winter	7-Feb-18	14-Feb-18				
	st. patrick	1963	11	7	1	summer	27-Jul-18	31-Jul-18	4	101 (5)	4	105 (5)
					2	summer	7-Aug-18	9-Aug-18				
	york mills	1973	12	5	1	summer	16-Aug-18	28-Aug-18	5	147 (12)	5	157 (10)
line 2	bathurst	1966	8	4	1	spring	4-Apr-18	11-Apr-18	13	240 (44)	13	182 (25)
					2	summer	11-Jul-18	18-Jul-18				
	bloor-yonge	1954	6	0	1	winter	12-Dec-17	18-Dec-17	14	357 (66)	14	260 (42)
					2	winter	29-Dec-17	7-Jan-18				
	castle frank	1966	7	1	1	winter	12-Dec-17	18-Dec-17	14	300 (76)	14	256 (43)
					2	winter	29-Dec-17	7-Jan-18				
	christie	1966	7	3	1	spring	4-Apr-18	11-Apr-18	13	357 (80)	12	218 (37)
					2	summer	11-Jul-18	18-Jul-18				
	coxwell	1966	9	3	1	winter	2-Mar-18	8-Mar-18	7	476 (102)	7	259 (33)
	dufferin	1966	8	2	1	summer	13-Jul-18	19-Jul-18	4	406 (83)	4	209 (50)
	main street	1968	10	1	1	winter	2-Mar-18	8-Mar-18	7	497 (86)	7	287 (16)
	old mill[d]	1968	7	0	1	winter	22-Feb-18	28-Feb-18	12	395 (132)	12	247 (37)
	ossington	1966	9	3	1	spring	4-Apr-18	11-Apr-18	14	238 (47)	14	181 (33)
					2	summer	11-Jul-18	20-Jul-18				
	sherbourne	1966	7	1	1	winter	12-Dec-17	18-Dec-17	14	357 (81)	14	266 (37)
					2	winter	29-Dec-17	7-Jan-18				
	woodbine	1966	8	2	1	winter	2-Mar-18	8-Mar-18	7	432 (96)	7	249 (23)
outdoor[e]	200 College	-	-	-	-	spr&sum	10-May-18	23-Aug-18	12	10 (2)	12	9 (2)
	4905 Dufferin	-	-	-	-	spr&sum	8-Jun-18	23-Aug-18	11	9 (3)	11	6 (2)

[a]distance to an above-grade section of the system; [b]session #; [c](μg/m3); [d]two platform positions sampled in parallel; [e]seven-day samples.

This large difference between $PM_{2.5}$ of line 1 and line 2 has been discussed previously (Van Ryswyk et al., 2021). Breifly, this differed from the relatively similar $PM_{2.5}$ concentrations in the two lines measured in 2010–2011. This change was due to several factors. A modernization of line 1 rolling stock contributed to the 30% reduction in $PM_{2.5}$ throughout that line. On line 2, an issue involving an increase in the frequency of friction-brake use and wheel flats resulted in a significant increase of $PM_{2.5}$. A line-wide reduction in $PM_{2.5}$ concentrations was also noted after its resolution in 2019. The friction brake/wheel flats issue on line 2 persisted throughout this study's 9-month sampling campaign. The increase in subway-sourced PM emission was more evident in the fine particle size range. Data collected in the 2010–2011 study measured a system-wide $PM_{2.5}$:$PM_{2.5\text{-}10}$ ratio of ~ 0.5 data (Van Ryswyk et al., 2017). In 2017–2018 the ratio was 0.93 on line 1 and 1.55 on line 2 (Table S2). This suggests that the rise in PM on line 2 which resulted from the increase in emissions from brakes, wheels, and rails was more pronounced in the fine mode. Finally, concentrations of $PM_{2.5}$ and $PM_{2.5\text{-}10}$ on subway platforms were observed to be over an order of magnitude higher than outdoors (Fig. 3) as has been observed in many other systems (Moreno and de Miguel, 2018; Xu and Hao, 2017).

3.2. Physiochemical characterization of $PM_{2.5}$: XRF, SEM, and XANES analyses

The majority of the 33 elements included in the XRF analysis were above detection (Table S3). Elements with over 80% of samples below detection included Ag, Cd, Ce, In, P, Sb, Se, and Ti. Two elements were found to be detectable on only one line (Pb on line 1 and

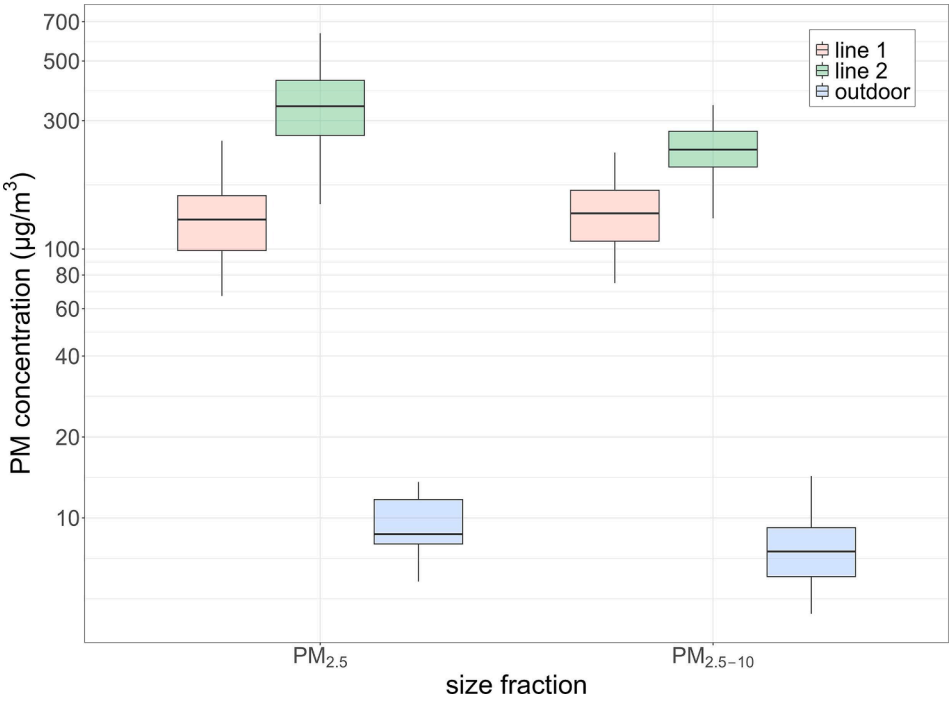

Fig. 3. Distribution of PM concentrations by size fraction and sampling environment (line 1, line 2, and outdoor sites).

V on line 2). The SEM image of the single sample suggests amorphous particles < 2 μm in diameter to be common (Figure S1). Results of the XANES analysis (conducted on 1–2 samples from each station, n = 30) for Fe, Cr, Cu, Mn, Ni, and Zn are presented in Table S4A&B. Each of these elements were found to be extensively in an oxide or sulfide form. Mixed Fe(II)/Fe(III) oxide magnetite (Fe_3O_4) was the most common iron oxide on both lines followed by Fe(III) oxides hematite (α-Fe_2O_3) and goethite (FeOOH). Both Fe(III) species have similar Fe K-edge XANES lineshapes and produced similar results in the LCF analysis, suggesting that both are likely present. Ferrihydrite ($FeO•0.5(H_2O)$) was observed only at the Museum station of line 1. There was no evidence of maghemite (γ-Fe_2O_3). Qualitative analysis of the Cr K-edge XANES spectra indicated that Cr(III) was the only oxidation state present. This is a significant finding for future evaluation of the health effects of subway $PM_{2.5}$ as Cr(VI) is a strong carcinogen and has as higher toxicity than Cr(III) (US EPA, 2009). Copper (II) oxide (CuO) was slightly more common than copper (I) oxide (Cu_2O) and, combined, accounted for 0.2% of $PM_{2.5}$ mass on each line. Manganese was observed to be Mn(II) and Mn(III) oxides. The two major zinc species were zinc sulfide (ZnS) and zinc oxide. Ni K-edge XANES analysis identified two major nickel species: Nickel (II) sulfide (NiS) and Ni(II) oxide. XANES analysis suggested that Mn, Ni(II), and Zn(II) oxides were amorphous in nature and possibly associated with iron. Tests against Co standards were not successful owing to interference from the high Fe concentration.

The composition profile of $PM_{2.5}$, based on the XRF and XANES analyses is presented in Fig. 4. On each line, ~82% of the $PM_{2.5}$ composition was accounted for by the species measured with iron oxides accounting for the majority of $PM_{2.5}$ mass. Magnetite, the most common Fe oxide, accounted for 57.5% and 67.5% of the mass on lines 1 and 2, respectively with other iron oxides contributing 18.6% (line 1) or 6.2% (line 2). In descending order, 6.9% of the line 1 $PM_{2.5}$ was composed of 1.2–0.1% Ba, S, Cl, Si, Ca, Al, Na, Mn, Cr_2O_3, Cs, Zn, CuO, Cu_2O, Mg, Co, and K. Concentrations of P, Sb, Sr, Sn, Br, Ag, Ni, and Zr each accounted for < 0.1% of $PM_{2.5}$ mass. Line 2 $PM_{2.5}$ was 3.4–0.1% (in descending order) Ba, Cl, S, Ca, Si, Al, Mn, Cr_2O_3, Na, Cs, Zn, Co, CuO, Cu_2O, K, and Sr with V, As, Mg, Ni, Sn, Zr, Sb, Rb, and Br each comprising less than 0.1% of $PM_{2.5}$ mass.

Evidence of subway PM being extensively oxidized has been noted in the systems of Barcelona (Querol et al., 2012, Moreno et al., 2015), Shanghai (Lu et al., 2015), and Seoul (Eom et al., 2013). In Barcelona, the bulk of the Fe was observed to be in the oxidized form of hematite (Querol et al., 2012) as well as magnetite (Moreno et al., 2015). In the Shanghai subway system, the XANES spectra of Fe-$PM_{2.5}$ resembled that of Fe_2O_3, suggesting hematite or maghemite. A conceptual model for this extensive oxidation of subway-sourced PM was proposed by Moreno et al., (2015), outlining the formation of subway-sourced PM from the wear and friction of braking. In this model, the active surfaces of the planar and flake-like morphology of subway-sourced PM can undergo rapid oxidization by ambient oxygen to magnetite, followed by successive oxidation to maghemite and then hematite. This suggests that $PM_{2.5}$ in the Toronto subway is freshly emitted as magnetite was the predominant Fe oxide.

The Ba is mostly likely present as $BaSO_4$ as was noted in the PM from the Tokyo subway (Furuya et al., 2001) and observed in SEM imagery of subway PM_{10} (Moreno et al., 2015). It is likely that some of the remaining uncharacterized mass (~18% of the $PM_{2.5}$) was also due to oxygen in metal oxides and sulfate in $BaSO_4$ present in brake PM. Elemental carbon, which was not analysed in this study,

may also account for a proportion of the uncharacterized PM. However, the carbon content of subway PM in the Toronto subway is likely less than what has been observed in other systems which use electrification with carbon components and continual ventilation which introduces outdoor-sourced carbon. For example, scanning electron microscopy of PM_{10} from the Barcelona subway noted carbon as diesel soot infiltrated from outdoor air (Moreno et al., 2015). The Barcelona subway system uses graphite pantographs in the catenary-pantograph electrical system which was also noted as a source of carbon. The Toronto subway has a third line electrification system which uses conductor or contact rails and shoes which are mostly iron in composition (see section 3.3).

The high iron oxide content (75% and 73% of $PM_{2.5}$ mass on line 1 and 2, respectively) indicates a large proportion of the subway $PM_{2.5}$ originating from the system itself (Chillrud et al., 2004; Cusack et al., 2015; Grass et al., 2010; Martins et al., 2016; Minguillón et al., 2018; Park et al., 2014a; Park et al., 2012). High correlations between alloying elements used in steel production are also observed in $PM_{2.5}$ samples from each line (Figure S2). This is also supported by comparing the XRF results of the subway and outdoor $PM_{2.5}$ samples (Fig. 5). For each of the elements presented, subway levels are significantly higher than outdoor. The closest elemental concentration between outdoor and subway was K which was four times higher on line 1 platforms than outdoors. This is in contrast with other systems. In the Shanghai subway, where $PM_{2.5}$ was simultaneously sampled on the platforms and at the above ground outdoor air at three stations, mass concentrations of Ca, Al, and Zn were found to be higher in outdoor air (Lu et al., 2015). In the Barcelona subway, fine-fraction elemental concentrations such as Al, Co, total carbon, and others were more comparable to outdoor

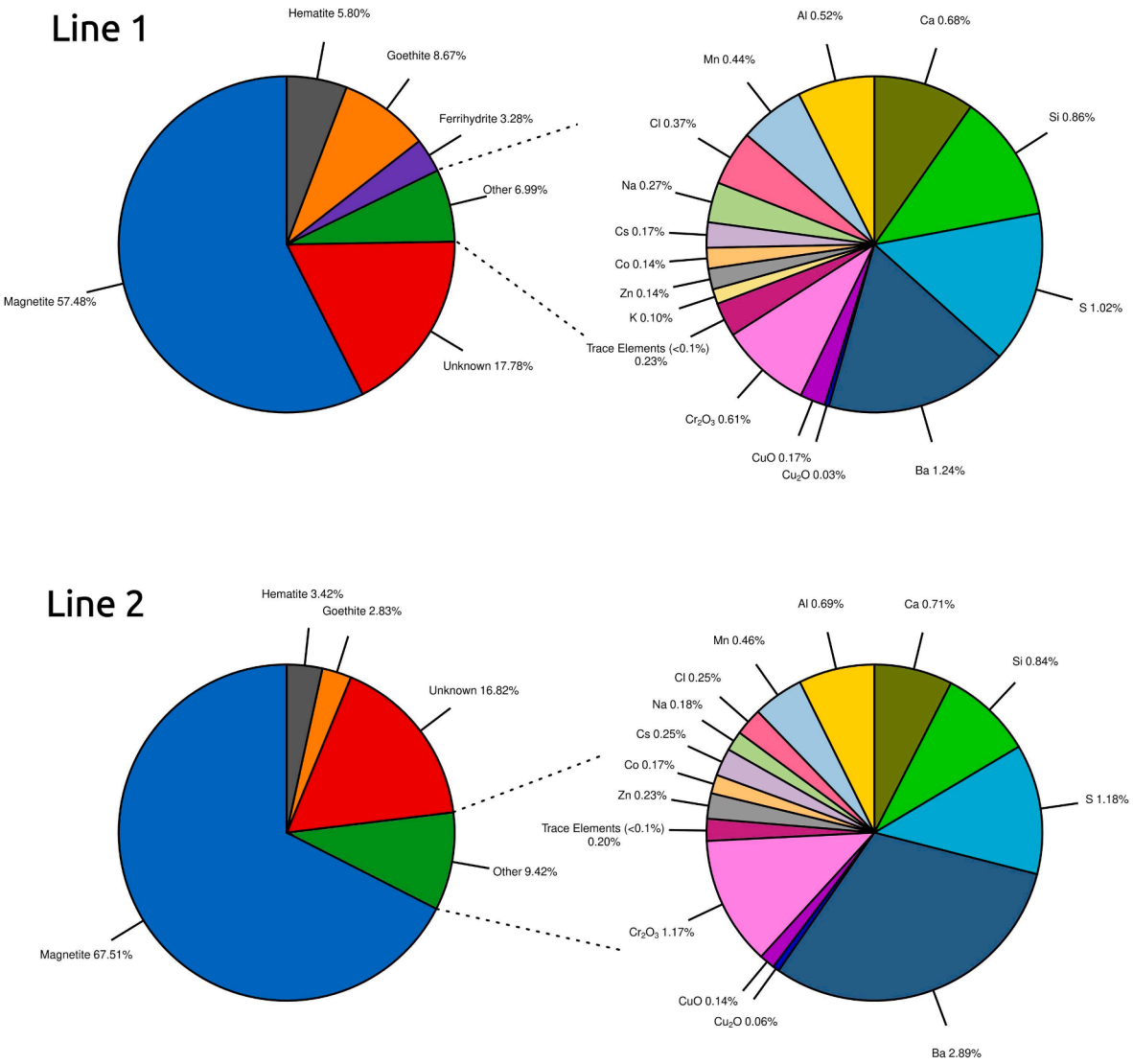

Fig. 4. Composition of platform $PM_{2.5}$ by XRF and XANES (Fe, Cr, & Cu). Top: Line 1, n = 82 samples, 11 stations, μ(SD) = 122(30) μg/m^3. Bottom: Line 2, n = 119 samples, 11 stations, μ(SD) = 369(85) μg/m^3.

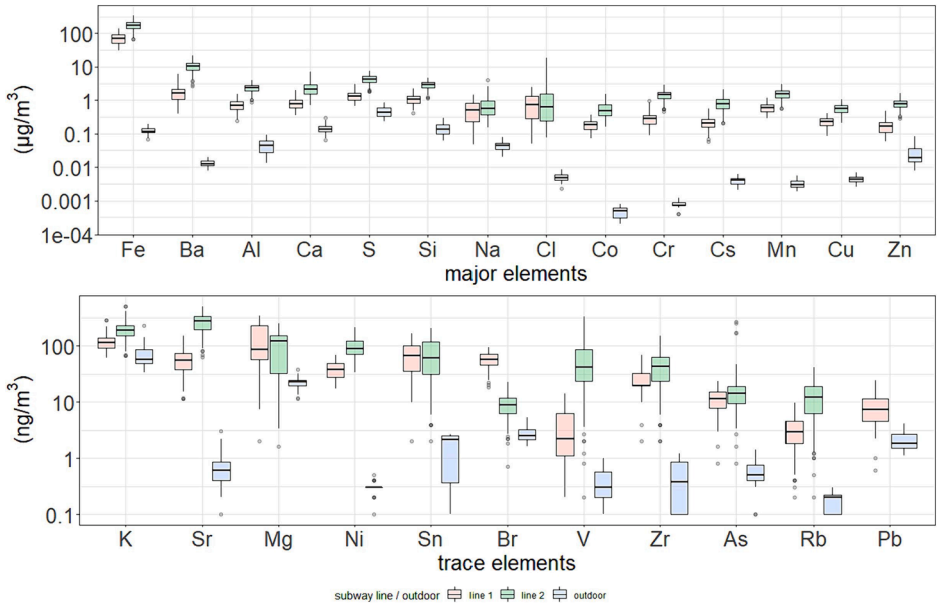

Fig. 5. Concentrations of major (above panel) and trace (lower panel) elements in line 1, line 2, and outdoor $PM_{2.5}$.

levels (Minguillón et al., 2018). Accordingly, of the ten $PM_{2.5}$ sources identified for the Barcelona system, four were of outdoor origin. In this study, the higher subway concentrations of all fine-fraction elements, which accounts for ~ 82% of mass, suggests that in Toronto, most of the $PM_{2.5}$ originates from within the system. Differences of the mass concentrations of fine fraction metals between lines is also indicative of their subway origin. For example, the higher Fe on line 2 is on account of the higher emission of subway PM from the aforementioned friction brake/wheel flat issue. Most other elements share this trend as well (Ba, Al, Ca, S, Si, Co, Cr, Cs, Mn, Zn, Cu, K, Sr, Ni, Rb, As, and V), suggesting their origins to also be related to subway operation rather than from inflow of outdoor air. There were some exceptions to this trend; higher concentrations were observed on line 1 for a few elements, despite the overall higher mass concentration of $PM_{2.5}$ on line 2. Line 1 had higher Br and its stations were the only platforms with detectable levels of Pb. With these elements having higher concentrations than outdoor, this suggests an unidentified subway source specific to line 1. Elements which were relatively equal between lines included Na, Cl, Mg, Zr, and Sn. Overall, there is little evidence of an outdoor $PM_{2.5}$ contribution to the $PM_{2.5}$ in this subway system.

3.3. *Comparison of elemental composition of subway components*

With evidence pointing to the subway platform $PM_{2.5}$ being mostly system-sourced, the subway component material specifications (wheels, rails, contact rails and contact shoes) and the XRF analyses of line 1 and line 2 brake pads represented the main resource for the identification of source markers. This elemental composition information (i.e., 'maximum % by weight') is summarized in Table S5 for running rails, wheels, contact rails, and contact shoes. The Fe ratios for elements measured in the line 1 and line 2 brake pad samples are also presented. Overall, 16 elements were identified in at least one subway system component. The elements listed for each component are not comprehensive as the specification documents are proprietary and the suite of analytes include in the XRF analysis of brake pad material may not cover all elements included in their fabrication. Further, the compositional data from these sources may not reflect what would be emitted in the $PM_{2.5}$ size fraction. However, while this list of subway components which may emit PM is not exhaustive, they are considered the main components which undergo frictional forces on a regular basis and have been repeatedly identified as important in the literature on subway-sourced PM (Huang et al., 2021; Martins et al., 2016; Minguillón et al., 2018; Park et al., 2014a; Park et al., 2012). Ballast was not considered as a source as there is no ballast in the below-grade sections of line 1 and 2 of the Toronto subway. Comparisons between the content of brake pads and the other subway components was complicated by an inconsistency in metrics. While the composition of brake pads is in Fe ratios, the elemental content of the other components from the specifications is provided in 'maximum % by weight'. However, as can be seen in Table S5, the wheels, running rails, contact rails, and contact shoes are > 94% Fe. Therefore, their 'maximum % by weight' data are a good approximation of Fe ratios and can thus be compared to the composition of the brake pad samples.

Overall, an examination of Table S5 reveals the brake pad material to be distinct from other subway components, which are mainly Fe in content (>94% by weight). Of the elements identified in the brake pad material, Ba had the highest Fe ratio (Ba:Fe ratios of 0.37 and 0.12 for line 1 and line 2, respectively). Ba is a common component of car and truck brake lining material (Grigoratos and Martini, 2015) and has also been observed in the particles emitted from train disc brake pads (Abbasi et al., 2012). As Ba was not listed in the material specification of other subway components, it was designated as the main marker of the brake pad source. The Ba content of the platform $PM_{2.5}$ samples was compared to other elements found to be abundant in the brake pad samples. Comparisons were conducted

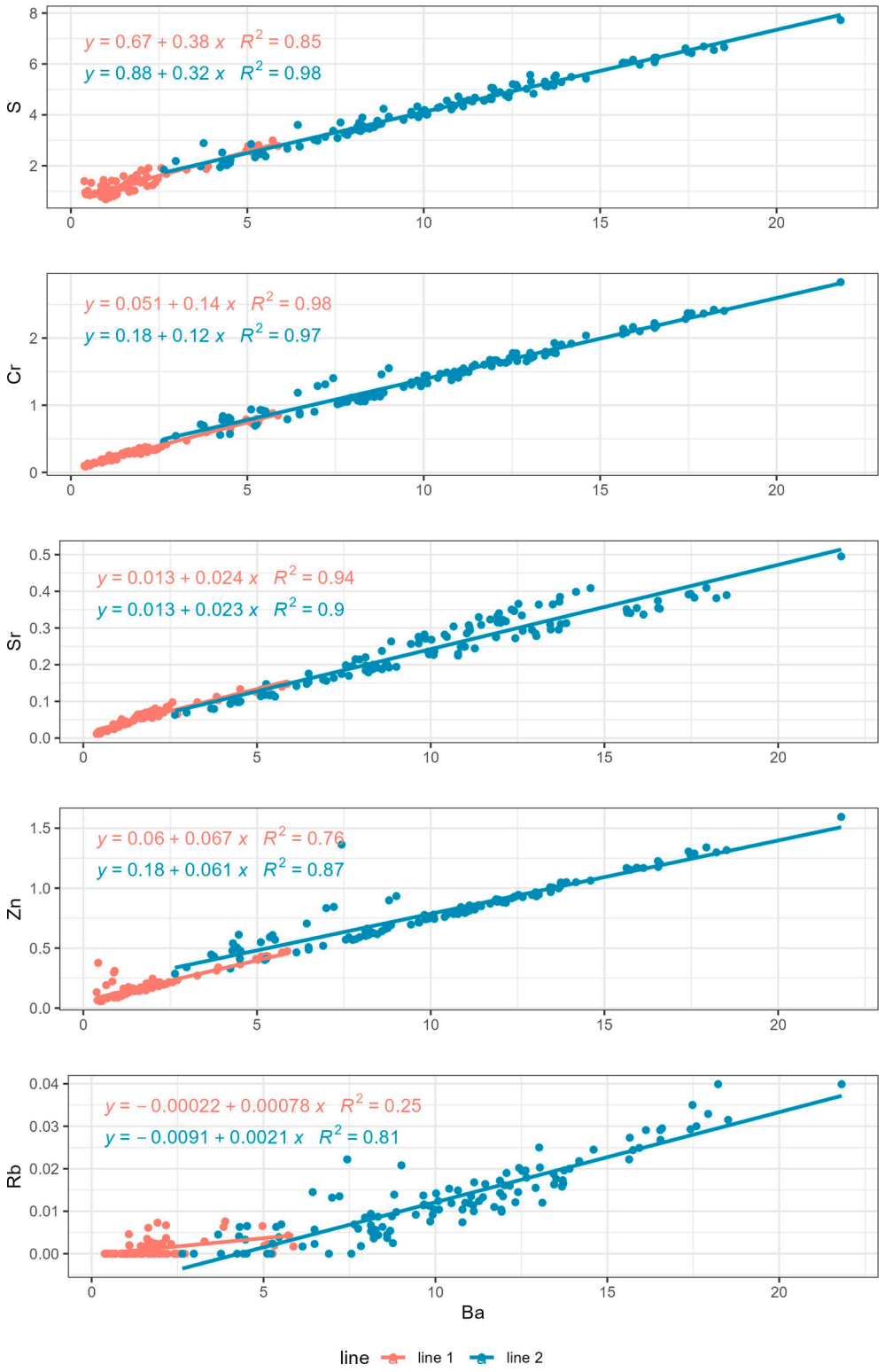

Fig. 6. Relationship of elemental components of subway $PM_{2.5}$ on line 1 and 2; line-stratified least-squared regression analyses between S, Cr, Sr, Zn, and Rb with the brake marker 'Ba' (ng/m^3).

using scatterplots and least-squared regression (LSR) analyses and stratified by line. With this approach, the elements Sr, Cr, S, Zn, and Rb were found to be highly correlated with Ba ($R^2 > 85\%$ on at least one line) implying a common single source for these elements (Fig. 6). Rubidium was not listed in the specification or available in the Xact analyses of brake pads, however, it is used in some brake pads (Bashir et al., 2019; SWDE, 2011). As the Ba scatterplots of other elements Ca, K, and Pb (not presented) indicated a second source, they were designated as markers of 'multiple subway components'. The elements Al, Mn, Cu, Si, Ni and V were listed in several components, some with similar Fe ratios. Accordingly, they were also designated as markers of 'multiple subway components'. Sn was unique to contact rails. Contact shoes were also noted to contain Sn in the Stockholm subway system, which also features a third rail electrification system (Cha et al., 2016). Therefore, Sn was assigned as a marker of 'contact rail & shoes'.

3.4. Positive Matrix Factorization of $PM_{2.5}$

A total of 22 elemental species were included in the PMF analysis. Elements which were > 80% below detection and/or had insufficient sensitivity (signal to noise ratio < 0.2) included Ag, Cd, Ce, In, P, Pb, Sb, Sn, Se, Ti, and V and were not included in the PMF. This information is summarized in the Supplemental Information along with mean estimates of precision values used in the PMF analyses (Table S6). Fe was converted to FeO by summing the mass of all Fe oxides quantified by XANES. The other metals analysed by XANES (Cr, Cu, Mn, Zn, and Ni) were not converted as it would have a limited impact on the total mass represented in the PMF. The elements included in the PMF accounted for ~ 82% of $PM_{2.5}$ mass on both lines. A 3-factor solution gave the most reproducible Q (robust) figures relative to the 2 and 4–6 factor solutions. Bootstrap diagnostics demonstrated good reproducibility and there were no unmapped factors (Section 3 of Supplemental Information). Species used to characterize and interpret each of the three factors withstood error estimation modelling and showed very small DISP intervals.

Each PMF factor was subway-sourced as they were mainly composed of FeO (>84%; Fig. 7). They were similar in composition for the majority of the 22 elemental species included in the PMF model (Table S7). The exceptions were the marker groups FeO, Br + Cr, and Na + Cl. The marker FeO represented $PM_{2.5}$ sourced from the Fe-dominated subway components (Fe-DC). These included the wheels, running rails, contact rails, and contact shoes that were > 94% Fe in composition (Table S5). This marker was the main component of each of the three PMF factors, in varying proportion (94%, 90%, and 84%; Table S7). The marker group Ba + Cr represented markers of 'brake pads'. These elements were highly correlated (Fig. 6) and the most abundant components of the brake pads, next to Fe (Table S5). This marker group was present in the second and third PMF factor in similar proportions. The elements of the marker group Na + Cl were also highly correlated and represented a marker of 'road salt'. This marker group was present in the third PMF factor. Each source was labelled according to the presence of these marker groups. The PMF factor profiles are presented in Fig. 7, Table S7 and Table S8. PMF factor contributions to the sum of characterized $PM_{2.5}$ (~82% of the $PM_{2.5}$) are presented by station in Fig. 8 and line in Fig. 9.

PMF factor 1: 'Fe-DC' $PM_{2.5}$ source

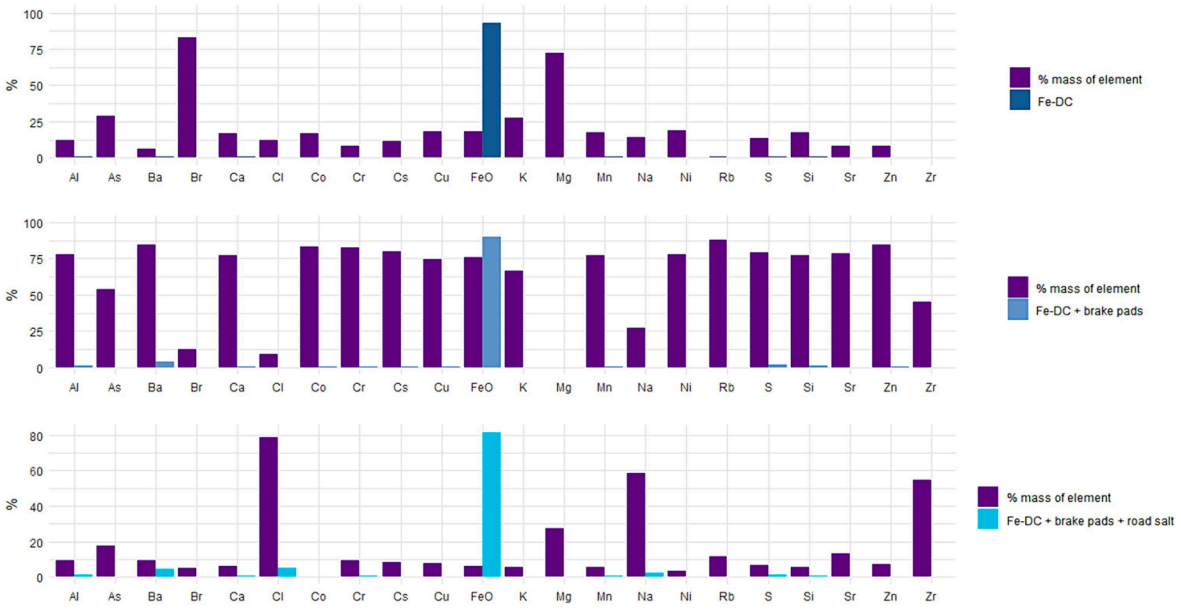

Fig. 7. Source profiles of subway $PM_{2.5}$ as determined by PMF.

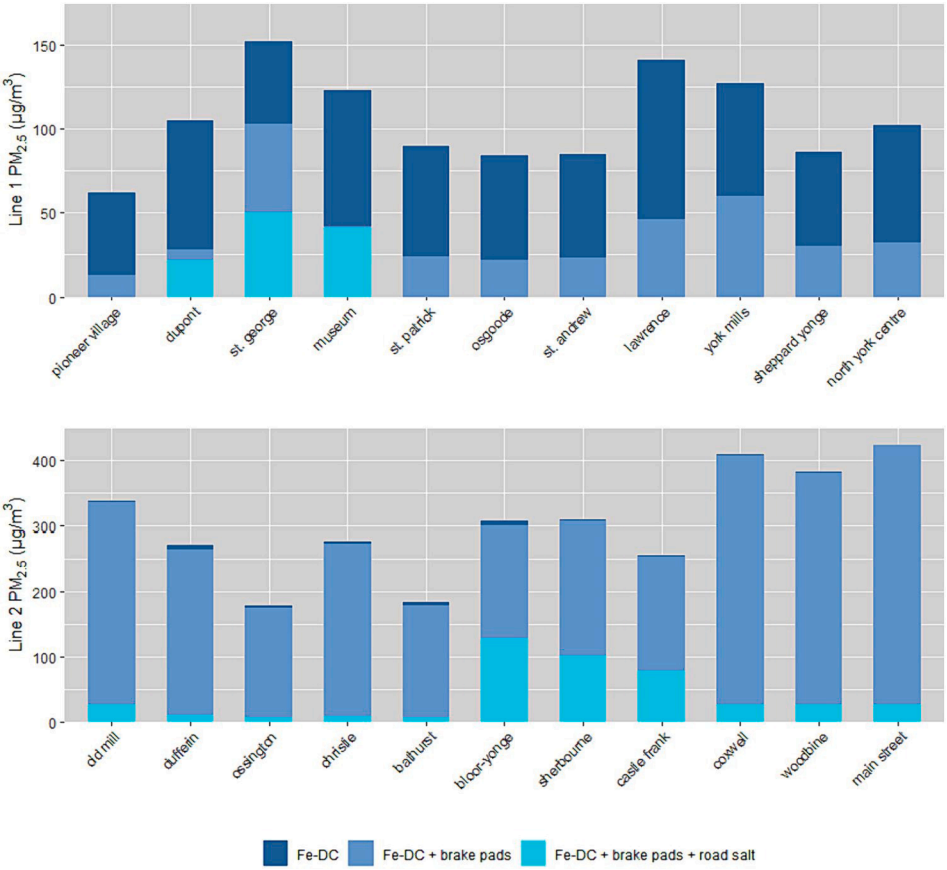

Fig. 8. Average source contributions by station and line.

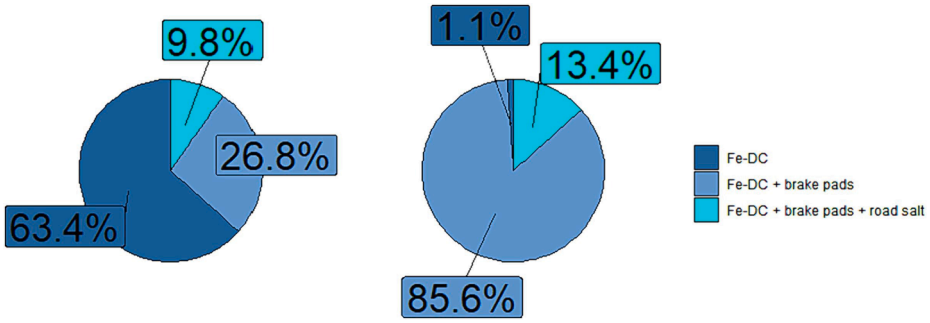

Fig. 9. Average source contributions on line 1 (left) and line 2 (right).

Source 1 was labelled after the marker 'Fe-DC' as FeO accounted for 94% of its mass and there were minimal amounts of the 'Ba + Cr' or 'Na + Cl' marker groups (Table S7). Based on the error estimation analysis (Table S7), the PMF analysis did not confidently estimate Ba or Cl to comprise a portion of this source. The lack of brake wear markers and the dominant FeO component suggest that $PM_{2.5}$ from this source resulted from steel-on-steel abrasion with minimal emission from brake pads. Emissions from the wheels, rails, contact wheels, and contact shoes would take place during system operations other than friction brake use (e.g., from abrasion of the steel wheels and rails and contact rails and shoes as trains travel between stations, during regenerative braking, and possibly the train motors and doors). This source accounted for the majority of $PM_{2.5}$ on line 1 (63.4%) and only 1.1% of $PM_{2.5}$ on line 2 (Fig. 9). This near exclusive presence on line 1 reflects the stark contrast of friction brake use between lines. While there was a high rate of friction brake use on line 2, friction brakes were only used at speeds < 5 km/h on line 1. The line-specific nature of this source may also be due to other trace elements. This source accounted for the majority of Mg and Br (Fig. 7) that was significantly higher on line 1 (Fig. 5). These elements were from a source (or sources) specific to line 1 as they were almost completely exclusive to line 1 stations (Figures S3 and S4). While they were grouped together in the PMF analysis, they were not correlated to each other within the samples on line 1 (p

~ -0.1; Figure S2). They were also positively correlated with FeO (Figure S2) suggesting they were related to a steel source.

PMF factor 2: 'Fe-DC + brake pads' $PM_{2.5}$ source

Source 2 was labelled 'Fe-DC + brake pads' as it was 90% FeO and 4% Ba + Cr, with minimal levels of Na + Cl. Based on the error estimation analysis (Table S7), the PMF analysis did not confidently estimate Cl to comprise a portion of this source. With the dominant FeO component and inclusion of the main markers of brake pads (Ba + Cr), this source reflects emissions from each of the main five subway components. It accounts for the majority of $PM_{2.5}$ sampled in the study contributing 26.8% of line 1 $PM_{2.5}$ (mean(SD):122(30) $\mu g/m^3$) and 85.6% of line 2 $PM_{2.5}$ (mean(SD): 369(85) $\mu g/m^3$). As the main source on line 2, it represents the profile of $PM_{2.5}$ resulting from subway operation with a high rate of wheel flats and friction brake use. This source was also present throughout line 1, albeit at a lower concentration, reflecting line 1′s normal use of regenerative braking, where friction brakes are only applied at speeds < 5 km/h. There were two line 1 stations (Dupont and Museum) with only trace amounts of this source. In these cases, the third source was present.

PMF factor 3: 'Fe-DC + brake pads + road salt' $PM_{2.5}$ source

Source 3 was labelled 'Fe-DC + brake pads + road salt' as it was 84% FeO, 4.8% Ba + Cr, and 5.0% Na + Cl. Road salt (NaCl) is used as a de-icing agent in many Canadian cities and has been observed to be a continual source of outdoor $PM_{2.5}$ in winter and spring in Toronto from 2004 to 2016 (Jeong et al., 2020). This might suggest that the NaCl was of outdoor origin. However, its presence in the subway air may not reflect the typical infiltration of outdoor air. Na and Cl were significantly higher in subways relative to outdoors (Fig. 5). As salt is applied in large amounts to the sidewalks outside stations as well as stairways into and bus platforms, the higher concentrations of these elements in subway $PM_{2.5}$ relative to outdoor $PM_{2.5}$ could be due to the introduction of road salt via passenger footwear rather than solely by the infiltration of outdoor air. As well, snow melt would contain road salt and drain into the subway. Combined, Na and Cl only accounted for ~ 5% of the mass of this source (Table S7). The remainder of its composition reflects that of the 'Fe-DC + brake pads' source. The separation of these two sources could be on account of our sampling campaign. The presence of the 'Fe-DC + brake pads + road salt' on line 1 is only observed at the stations sampled in winter, the rest having been exclusively sampled in July and August (summer). Had these stations been sampled in summer, Dupont and Museum would likely have a similar source profile as the other line 1 stations with ~ 60% being sourced from the 'Fe-DC' source and ~ 40% from the 'Fe-DC + brake pads' source. The St. George station is unique with contributions from all three sources. This is likely on account of it being a line1/line2 crossover station and being exclusively sampled in the winter. The result being a blend of line 1 and line 2 $PM_{2.5}$. On line 2, the concentrations of the 'Fe-DC + brake pads + road salt' source is highest at stations exclusively sampled in winter (Bloor-Yonge, Sherbourne, and Castle Frank).

Overall, the PMF analysis indicates that the main sources of subway $PM_{2.5}$ in this study are emissions from the rails, wheels, contact rails, contact shoes, and brake pads. While the PMF analysis identified three sources, none were specific to a single subway component. The 'Fe-DC' source represented four of these components while the remaining two sources represented all five. Accordingly, the three sources were very similar in composition. And, as the compositional data used in the PMF account for ~ 82% of the $PM_{2.5}$ mass, these results indicate a homogeneous subway-sourced $PM_{2.5}$ composition profile throughout this subway system. There are several factors which contribute to this; no outdoor $PM_{2.5}$ sources were identified suggesting limited air exchange with the outdoors; the composition of four of the five main subway components (wheels, rails, contact rails and contact shoes) were all mainly (>94%) Fe; and the concurrent and collocated emission of PM from these components.

The limited compositional differences between the three identified sources were due to differences in seasons and lines. The third source was identified on account of traces of road salt (Na + Cl) in samples collected in winter. In terms of line differences, there was a stark contrast in operating conditions between line 1 (the typical operating condition of only using friction braking at < 5 km/h) and line 2 (atypical high rate of friction braking and wheel flats) resulting in higher concentrations of the Ba and Cr brake markers in line 2 $PM_{2.5}$. Also, each line used different rolling stock with line-specific brake pads (which were different in composition; Table S5). Line-specific sources have also been identified by PMF in the Barcelona system (Minguillón et al., 2018). Source 'Brake A' was identified in stations of lines 'L1′ and 'L3′ and 'Brake B' on stations of line 'L4′. The chemical profiles of these sources and the brake pads of these lines was shown to be similar. In other source apportionment studies of subway PM, sample collection was limited to single lines (Huang et al., 2021; Park et al., 2014a; Park et al., 2012) preventing the identification of line-specific sources.

The impact of line and season on the PMF analysis is reflected in the relationship between Fe (the marker for the Fe-dominated components) and Ba (the main marker for brake pads). The relationship between Fe and Ba (slope of the lines on Fig. 10) differed between the two lines. The exception is the St. George station, which features its own Fe:Ba ratio. This is likely on account of it being a line 1 – line 2 crossover station resulting in a Fe:Ba ratio representing a blend of line 1 and line 2 $PM_{2.5}$. Seasonality is also evident in the Fe:Ba relationship of line 2 samples. The 'line 2 summer' group contains all line 2 samples collected in the summer. This artificial seasonality was likely driven by a change in the brake pads type being used on line 2. This supposition is supported by several observations. Three of the four line 2 stations sampled in the summer were also sampled in the winter-spring period. The mean(SD) $PM_{2.5}$ concentration of these stations were unchanged between winter and summer; Bathurst: 145(30) vs 135(29) $\mu g/m^3$; Christie: 211(43) vs 205(43) $\mu g/m^3$; and Ossington: 140(32) vs 137(23) $\mu g/m^3$. Therefore, the same amount of $PM_{2.5}$ emission was taking place in both sessions. The higher Fe:Ba ratio in summer could be explained by a decrease in the emission of $PM_{2.5}$ from brake pads. But, that would necessitate an increase in the emission from the Fe-dominated subway components (wheels, rails, and contact rails and shoes) resulting from a line-wide change in these components, which is unlikely. Therefore, the change in Fe:Ba ratio in the $PM_{2.5}$ on line 2 is most likely due to a change to a brake pad type with a different Fe:Ba ratio taking place between April and July 2018. The differences in Fe ratios for Ba by line and season is not shared by Ni and Mn (Fig. 10). For both Ni and Mn, the relationship with Fe is consistent across all

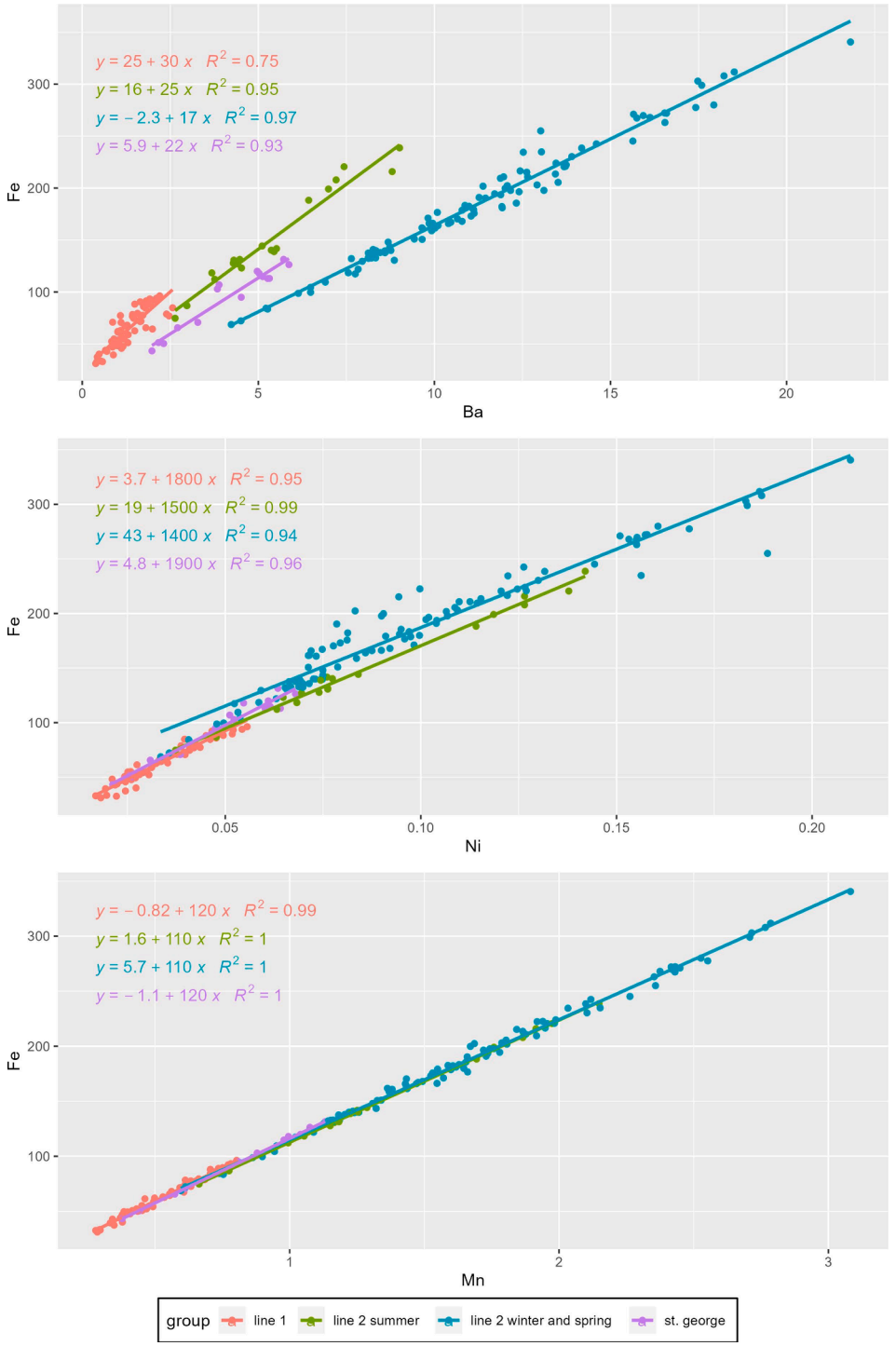

Fig. 10. Grouping of elemental correlations by line and season between Fe and Ba (top), Ni (middle), and Mn (bottom) (μg/m^3).

four of the aforementioned groups. As well, the high degree of correlation (Fe = Ni LSR $R^2 > 0.94$, Fe = Mn LSR $R^2 > 0.99$) suggests a single source for both these elements. However, as they are noted in multiple subway components (wheels, rails, contact rails, and contact shoes; Table S5), it is likely that PM emission from these subway components takes place concurrently.

3.5. Chemical mass balance analysis

The CMB approach afforded another opportunity to apportion platform $PM_{2.5}$ to specific subway components. However, the similarity of the four Fe-dominated subway components (Table S5) prevented CMB runs to converge when specifying source profiles for each individual component (n = 5). Therefore, a two-source approach was taken that grouped all Fe-dominated components (rails, wheels, contact rails, and contact shoes), the second source being brake pads. The two sources were represented solely by their Fe ratios for Fe (1.0 for both sources) and Ba (0 for the Fe-dominated components and 0.36 and 0.12 for the brake pads of line 1 and line 2, respectively (Table S5)). The CMB model analysis was stratified by line on account of the exclusive assignment of brake pads to the trains of each line. While the inclusion of elements was limited to only Fe and Ba in the CMB analysis, these two species accounted for ~ 76% of $PM_{2.5}$ on both lines. As well, Ba is exclusive to the brake pad material and the second most abundant element in the brake pads after Fe. Finally, many of the other components of $PM_{2.5}$ are tightly associated with Fe and/or Ba (Figure S2), which provides evidence of a similar source profile. The rationale for including only Fe and Ba in this analysis also allows for synthesis with the results of a subsequent analysis discussed in the next section.

The line-specific CMB models both estimated the proportion of $PM_{2.5}$ originating from the 'brake pad' source and the Fe-dominated components 'rails, wheels, contact rails and shoes' source (Fig. 11). The proportion of $PM_{2.5}$ being sourced from brake pads is far larger in line 2 (45%) relative to line 1 (8%), owing to the aforementioned elevated rate of friction brake use on that line. Like the PMF results, the apportionment between the two sources vary far more between lines then across stations within lines (Table S9). This speaks to factors of subway operation rather than station design affecting the level and composition of subway $PM_{2.5}$. For example, the high contribution of $PM_{2.5}$ from brake pads in line 2 is seen throughout the line 2 stations, while the lower proportion of brake pad-sourced $PM_{2.5}$ is equally as even throughout the line 1 stations. The only exception is line 1′s St. George station (a line1/2 crossover station) that displays a source profile between what is typical of each line. This line1/line2 'blend' is also demonstrated in the group-specific slopes of the Fe = Br regressions presented in Fig. 10. This is further evidence of the migration of the line 2 $PM_{2.5}$ to the line 1 platform, as discussed in this study's previous paper (Van Ryswyk et al., 2021). The amount of $PM_{2.5}$ originating from the steel components is also larger on line 2 suggesting the amount of $PM_{2.5}$ being sourced from wheels and rails is also increased. It is likely that the line 1 $PM_{2.5}$ source profile described in the CMB analysis is more typical of emissions in the Toronto system, when friction braking is only used once regenerative braking has slowed trains to 5 km/h. This suggests that while the process of braking is a substantial source, reducing emissions from the brake pads themselves, such as through alternate brake-pad composition, may not be the ideal target of mitigation measures.

3.6. Apportioning $PM_{2.5}$ by subway emission mechanisms

An *a posteriori* analysis was developed based on the results of the PMF and CMB results. Considering that the apportionment of subway $PM_{2.5}$ to single sources was complicated by the common composition of steel subway components (Table S5) and the concurrent and collocated nature of their emission, we explored the potential of considering subway-sourced $PM_{2.5}$ from the perspective of mechanisms rather than components. The predominantly system-sourced $PM_{2.5}$ in the Toronto subway enabled this analytical approach. The emission of subway-sourced PM results from several mechanisms involving high temperature frictional forces resulting in the ablation and abrasion of subway components (Moreno et al., 2015). These mechanisms can be grouped as those involving

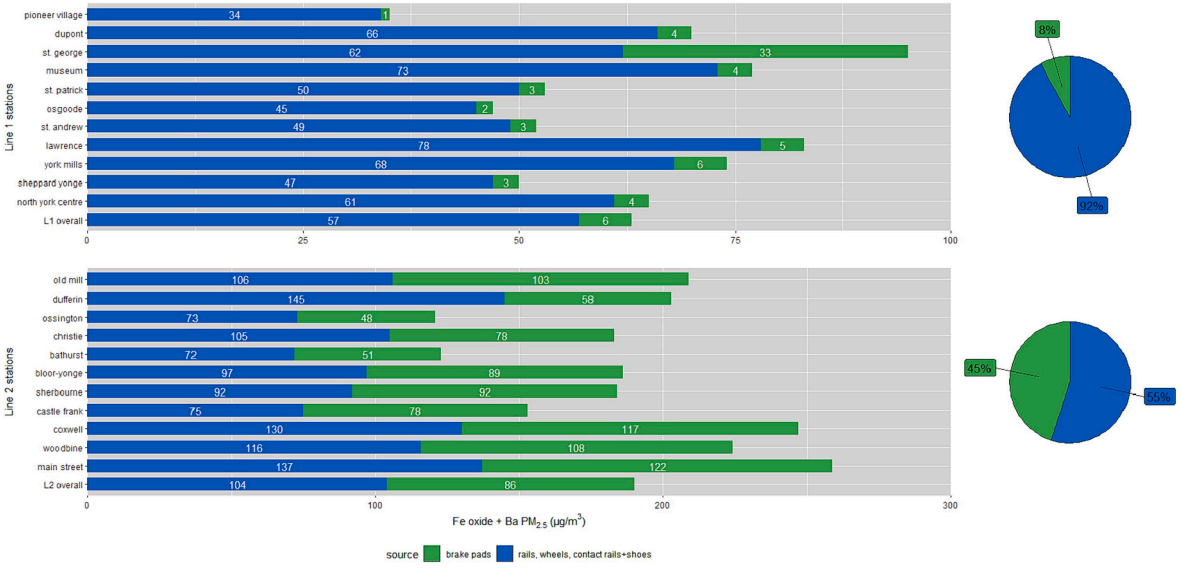

Fig. 11. Two-source ('brake pads' and 'rails, wheels, contact rail + shoes') CMB model for Fe and Ba $PM_{2.5}$.

Table 2
Source apportionment of subway $PM_{2.5}$-Fe+Ba to emission mechanisms by the synthesis of Fe=Ba total least squared regression (TLSR) and Chemical Mass Balance (CMB) analyses. $PM_{2.5}$-Fe+Ba is apportioned to three sources: wheels+rails from the Friction Brake Use (FBU) mechanism[a], brake shoes from the FBU mechanism, and Fe-DC[b] from the non-FBU mechanisms[c].

Line[d]	$PM_{2.5}$	TLSR		CMB		overall apportionment		
	μ (SD)	slope	y-int[e]	brake pads	Fe-DC	non-FBU	FBU	
		estimate (LCL, UCL)		mean % (min-max)		Fe-DC[f]	brake pads[g]	wheels+rails[h]
line 1	67 (17)	40 (36 - 45)	11 (6-17)	5% (4-8)	95% (92-96)	16%	5%	79%
line 2	219 (54)	17 (16 - 18)	-7 (-14–1)	49% (47-51)	51% (49-53)	0%	49%	51%

[a]FBU mechanism: friction brake use resulting in emissions from brake pads, wheels, and rails
[b]Fe-DC: Fe-dominated components: rails, wheels, contact rails and contact pads (>94% Fe; see Table S5)
[c]non-FBU mechanisms: regenerative braking, wheel:rail friction during cornering, and friction between contact rails & contact shoes
[d]St. George data excluded from line 1 (n=15); summer samples excluded from line 2 (n=19)
[e]The y-intercept represents the concentration of $PM_{2.5}$-Fe in the absence of $PM_{2.5}$-Ba (absence of FBU emissions).
[f]TLSR y-int / line $PM_{2.5}$ mean
[g]CMB result for brake pad-sourced $PM_{2.5}$
[h]100-(non-FBU+brakepads)

friction-brake use (FBU) and all other mechanisms (non-FBU). The FBU mechanism involves emissions from brake pads, wheels, and rails (n = 3 components). The non-FBU group includes mechanisms such as navigating curves, sliding events unrelated to braking, motor operation (during acceleration and regenerative braking), and the constant friction between the contact rails and contact shoes of the third rail electrification system. Emissions from this group are from rails, wheels, contact rails and contact shoes (n = 4 components).

In this analysis, Ba is the key marker of the FBU mechanism. It is abundant in and exclusive to brake pad material (Table S5). Therefore, the y-intercept of a $PM_{2.5}$-Fe = $PM_{2.5}$-Ba regression analysis provides an estimate of the amount of Fe that would be in the system in the absence of emissions related to FBU. To estimate this y-intercept, a total least squares regression (TLSR) was applied to account for the error in the x term (Ba) as well as the y term (Fe). Samples for summer on line 2 and line 1′s St. George station were excluded as these groups are limited in sample size and have Fe:Ba relationships distinct from the other samples of their respective lines (Fig. 10).

The TLSR analysis and the CMB analysis both apply line-stratification and exclusively focus on the Fe and Ba components of $PM_{2.5}$. Therefore, the brake pad-sourced $PM_{2.5}$ estimate from the CMB analysis can be subtracted from the FBU-sourced $PM_{2.5}$ estimate from the TLSR analysis to further apportion the FBU-$PM_{2.5}$ between the brake pads and the other two components involved in FBU: the wheels and rails. Overall, the synthesis of the TLSR and CMB analyses apportion the sum of $PM_{2.5}$-Fe and $PM_{2.5}$-Ba between (1) brake pads during FBU, (2) wheels and rails during FBU, and (3) wheels, rails, contact rails, and contact shoes during non-friction brake use (non-FBU).

The results of the TLSR analysis and its synthesis with the CMB results are presented in Table 2. For line 1, the Fe = Ba TLSR y-intercept is 11 μg/m^3 (95%CI: 6–17). This significantly non-zero intercept is evidence of a contribution of non-FBU mechanisms to subway $PM_{2.5}$ on line 1. Therefore, 16% and 84% of line 1 $PM_{2.5}$ (mean(SD) = 67(17) μg/m^3) is sourced from non-FBU and FBU mechanisms, respectively. For line 2, the y-intercept is significantly negative −7 μg/m^3 (95%CI: −14 - −1). Although a counterintuitive result, this constitutes evidence that line 2 $PM_{2.5}$ (mean(SD) = 219(54) μg/m^3) is predominantly soured from the FBU mechanism, with minimal contributions from non-FBU mechanisms. Using the CMB estimates for brake pad-sourced $PM_{2.5}$ (line 1: 5% (min–max: 4–8%), line 2: 49% (min–max: 47–51%)), the $PM_{2.5}$-FBU component was further divided between brake pads (the CMB result) and wheels and rails (100% - (TLSR-nonFBU $PM_{2.5}$ + CMB-brake pad $PM_{2.5}$)). Based on these estimates, the majority of $PM_{2.5}$ on line 1 is sourced from wheels and rails during friction brake use (79%). On line 2, the dominant emissions source was the FBU mechanism, divided equally between the brake pads (49%) and the wheels and rails (51%). It is important to note that line 1 is likely the more representative source profile of subway $PM_{2.5}$ in this system as line 2 was undergoing issues with increased friction brake use and wheel flats during this study, which were resolved in 2019, resulting in line-wide decrease in the concentration of $PM_{2.5}$ (Van Ryswyk et al., 2021).

4. Conclusions

This study provides several insights on the nature of subway $PM_{2.5}$ composition and sources. It also provides the first in depth analysis for a system with limited mechanical ventilation use where the piston effect of moving trains is the main driver of ventilation.

1. As with many other such systems, concentrations of $PM_{2.5}$ were high relative to the range of published subway $PM_{2.5}$ concentrations (Moreno and de Miguel, 2018). Mean platform $PM_{2.5}$ on line 2 ranged from 238 to 497 μg/m^3 and 75–179 μg/m^3 on line 1. These concentrations were 8 to 50 times higher than outdoor (<10 μg/m^3). Further, approximately 76% of $PM_{2.5}$ on both lines was composed of Fe oxides, mainly magnetite.
2. No Cr(VI) was detected in the system. This is of importance in characterizing the health risks of subway $PM_{2.5}$.

3. The measured elemental speciation accounted for ~ 82% of the $PM_{2.5}$ mass. A portion of the remaining uncharacterized mass could be accounted for by oxygen, given that the results of the XANES analyses revealed Fe, Cu, Cr, Mn, Ni, and Zn to be extensively oxidized. This near complete PM chemical characterization of $PM_{2.5}$ lends weight to the source characterization findings.
4. The identification of three source profiles in the PMF analysis was due to factors of season and line-specific components and operation. The majority of the mass of each source was composed of Fe and reflected multiple subway components. This characterizes the $PM_{2.5}$ of this system as predominantly system-sourced with a relatively homogeneous composition throughout the system. The potential reasons for this give insight to the nature of subway $PM_{2.5}$ sources: 1) there were no evidence of outdoor $PM_{2.5}$ sources; 2) the composition of four of the five main subway components (wheels, rails, contact rails and contact shoes) were all mainly (>94%) Fe; and 3) the concurrent and collocated emission of PM from these components.
5. A mechanistic approach to apportion the $PM_{2.5}$ mass in combination with the CMB analysis indicated three major sources: emissions from wheels and rails during friction braking, emissions from brake pads during friction braking, and emission from all other mechanisms. Of these, emissions during friction braking was the major source on both lines. Wheels and rails during braking was found to be the largest source in line 1. In line 2, where friction braking was being used at higher train speeds, there were comparable emissions from the brake pads, and the wheels and brakes.
6. The lower platform $PM_{2.5}$ concentrations of line 1 (75–179 $\mu g/m^3$) relative to line 2 (238–497 $\mu g/m^3$) and lower contribution of brake pads (5% vs 51%, respectively) emphasize the potential of regenerative braking systems to improve subway air quality.
7. Brake pad emissions can be < 10% of $PM_{2.5}$ on lines with regenerative braking systems that restrict friction brake use to speeds < 5 km/h. This is in contrast with findings in the Barcelona system where brake dust contributed 15–35% of $PM_{2.5}$ on lines 1 and 3 and 36–52% on line 4 (Minguillón et al., 2018).

Our conclusion that the subway $PM_{2.5}$ is predominantly system-sourced could be further strengthened by measures of station-specific air exchange rates. Outdoor sources contribute more to $PM_{2.5}$ in subway systems with the higher air exchange rates where regular mechanical ventilation is used (Minguillón et al., 2018; Moreno et al., 2017b) and in cities with higher outdoor $PM_{2.5}$ concentrations (Huang et al., 2021). Outdoor $PM_{2.5}$ concentrations in Toronto are generally lower than in many major cities, also contributing to our finding of no outdoor sources to subway $PM_{2.5}$. Further, due to this relatively low concentration of outdoor PM, air exchange simply results in the dilution of subway-sourced $PM_{2.5}$, preserving the overall compositional profile of $PM_{2.5}$ in the system. Therefore, the question of the PM-diluting capacity of the piston effect remains open. Research on this question suggests this capacity is more effective via tunnel openings than draught relief shafts and limited to within 3 km of tunnel openings (Van Ryswyk et al., 2017; Kappelt et al., 2022). Lastly, air exchange rates could have enabled the quantification of emission rates of subway-sourced $PM_{2.5}$. Based on our findings, implementing methods to reduce braking intensity and frequency, through automated control for example, appears to be the best opportunity to reduce emissions. The metallurgy and resulting performance of wheels and any replacement rails can also influence emissions. Finally, brake pad material combinations which emit less PM could also have benefits to reducing subway PM, in particular when more frequent friction braking occurs as was the case on line 2. There may be potential in exploring substitutes for the conventional materials of subway components as they have been shown to modify into soluble and toxic componts via their emission from frictional forces (Font et al., 2019). Methods of PM removal such as ventilation and filtration can also reduce the concentrations arising from the remaining emissions (Moreno et al., 2017b). The associated energy costs might be reduced by targeting stations with the highest PM concentrations and highest usage by passengers. Lastly, our finding of near mutually exclusive composition of subway and outdoor PM samples concurrently collected may support future comparison of the in vitro toxicities between outdoor and subway PM, an essential research question for the assessment of the health risks of subway $PM_{2.5}$.

CRediT authorship contribution statement

Keith Van Ryswyk: Writing – review & editing, Writing – original draft, Visualization, Validation, Resources, Project administration, Methodology, Investigation, Funding acquisition, Formal analysis, Data curation, Conceptualization. **Ryan Kulka:** Writing – review & editing, Writing – original draft, Validation, Resources, Project administration, Methodology, Investigation, Funding acquisition, Conceptualization. **Cheol-Heon Jeong:** Writing – original draft, Visualization, Software, Methodology, Investigation, Formal analysis, Data curation, Conceptualization. **Angelos T. Anastasopolos:** Writing – original draft, Visualization, Validation, Software, Methodology, Formal analysis, Data curation, Conceptualization. **Tim Shin:** Validation, Software, Resources, Methodology, Formal analysis, Conceptualization. **Peter Blanchard:** Visualization, Validation, Software, Methodology, Formal analysis, Data curation. **Danielle Veikle:** Visualization, Validation, Resources, Methodology, Investigation, Formal analysis, Data curation. **Greg J. Evans:** Writing – review & editing, Writing – original draft, Validation, Supervision, Resources, Project administration, Methodology, Investigation, Funding acquisition, Formal analysis, Conceptualization.

Declaration of competing interest

The authors declare that they have no known competing financial interests or personal relationships that could have appeared to influence the work reported in this paper.

Acknowledgements

This work was funded by the Government of Canada's Addressing Air Pollution Horizontal Initiative and supported by Health

Canada, the University of Toronto, and the Toronto Transit Commission. The authors thank Dr. Burke Barlow for their help in carrying out measurements at the Electron Imaging and Microanalysis Laboratory (EIML) at the Canadian Light Source (CLS). The authors would also like to acknowledge the contributions of Sarah Maleska, Laurent Frion, Kathleen Eng, Luckshya Meta, Phillip Lam, Philip K. Hopke, as well as the reviewers for their insightful comments.

Appendix A. Supplementary data

Supplementary data to this article can be found online at https://doi.org/10.1016/j.trd.2024.104164.

References

Abbasi, S., Olander, L., Larsson, C., Olofsson, U., Jansson, A., Sellgren, U., 2012. A field test study of airborne wear particles from a running regional train. Proc. Inst. Mech. Eng., Part f: J. Rail Rapid Transit 226 (1), 95–109. https://doi.org/10.1177/0954409711408774.

Azad, S., Luglio, D.G., Gordon, T., Thurston, G., Ghandehari, M., 2023. Particulate matter concentration and composition in the New York City subway system. Atmos. Pollut. Res. 14 (6), 101767 https://doi.org/10.1016/j.apr.2023.101767.

Bachoual, R., Boczkowski, J., Goven, D., Amara, N., Tabet, L., On, D., Leçon-Malas, V., Aubier, M., Lanone, S., 2007. Biological effects of particles from the paris subway system. Chem. Res. Toxicol. 20 (10), 1426–1433. https://doi.org/10.1021/tx700093j.

Bashir, M., Qayoum, A., Saleem, S.S., 2019. Influence of lignocellulosic banana fiber on the thermal stability of brake pad material. Mater. Res. Express 6, 115551.

Cha, Y., Hedberg, Y., Mei, N., Olofsson, U., 2016. Airborne wear particles generated from conductor rail and collector shoe contact: influence of sliding velocity and particle size. Tribol. Lett. 64 (3), 1–20. https://doi.org/10.1007/s11249-016-0775-7.

Chillrud, S., Epstein, D., Ross, J., Sax, S., Pederson, D., Spengler, J., Kinney, P., 2004. Elevated airborne exposures of teenagers to manganese, chromium, and iron from steel dust and New York City's subway system. Environ. Sci. Tech. 38 (3), 732–737.

Committee on the Medical Effects of Air Pollutants (COMEAP). Particulate Air Pollution on London Underground: Health Effects, Jan 9, 2019.https://www.gov.uk/government/publications/particulate-air-pollution-on-london-underground-health-effects.

Cusack, M., Talbot, N., Ondráček, J., Minguillón, M., Martins, V., Klouda, K., Schwarz, J., Ždímal, V., 2015. Variability of aerosols and chemical composition of PM10, PM2.5 and PM1 on a platform of the Prague underground metro. Atmos. Environ. 118, 176–183.

Eom, H., Jung, H., Sobanska, S., Chung, S., Son, Y., Kim, J., Sunwoo, Y., Ro, C., 2013. Iron speciation of airborne subway particles by the combined use of energy dispersive electron probe X-ray microanalysis and Raman microspectrometry. Anal. Chem. 85 (21), 10424–10431.

Font, O., Moreno, T., Querol, X., Martins, V., Sánchez Rodas, D., de Miguel, E., Capdevila, M., 2019. Origin and speciation of major and trace PM elements in the barcelona subway system. Transp. Res. Part D: Transp. Environ. 72 (April), 17–35. https://doi.org/10.1016/j.trd.2019.03.007.

Furuya, K., Kudo, Y., Okinagua, K., Yamuki, M., Takahashi, K., Araki, Y., Hisamatsu, Y., 2001. Seasonal variation and their characterization of suspended particulate matter in the air of subway stations. J. Trace Microprobe Techn. 19 (4), 469–485.

Grass, D.S., Ross, J.M., Family, F., Barbour, J., James Simpson, H., Coulibaly, D., Hernandez, J., Chen, Y., Slavkovich, V., Li, Y., Graziano, J., Santella, R.M., Brandt-Rauf, P., Chillrud, S.N., 2010. Airborne particulate metals in the New York City subway: a pilot study to assess the potential for health impacts. Environ. Res. 110 (1), 1–11. https://doi.org/10.1016/j.envres.2009.10.006.

Grigoratos, T., Martini, G., 2015. Brake wear particle emissions: a review. Environ. Sci. Pollut. Res. 22 (4), 2491–2504. https://doi.org/10.1007/s11356-014-3696-8.

Huang, S., Chen, P., Hu, K., Qiu, Y., Feng, W., Ren, Z., Wang, X., Huang, T., Wu, D., 2021. Characteristics and source identification of fine particles in the Nanchang subway. China. Build. Environ. 199, 107925 https://doi.org/10.1016/j.buildenv.2021.107925.

Jeong, C.-H., Traub, A., Huang, A., Hilker, N., Wang, J.M., Herod, D., Dabek-Zlotorzynska, E., Celo, V., Evans, G.J., 2020. Long-term analysis of PM2.5 from 2004 to 2017 in Toronto: composition, sources, and oxidative potential. Env Poll. 263 (B), 114652. Dio : 10.1016/j.envpol.2020.114652.

Kappelt, N., Russell, H., Fessa, D., Van Ryswyk, K., Hertel, O., Johnson, M., 2022. Particulate air pollution in the Copenhagen Metro Part 1: Mass concentrations and ventilation. Environ. Int. 107621.

Kim, G.S., Son, Y.S., Lee, J.H., Kim, I.W., Kim, J.C., Oh, J.T., Kim, H., 2016a. Air pollution monitoring and control system for subway stations using environmental sensors. J. Sensors. https://doi.org/10.1155/2016/1865614.

Kim, M.J., Braatz, R.D., Kim, J.T., Yoo, C.K., 2016b. Economical control of indoor air quality in underground metro station using an iterative dynamic programming-based ventilation system. Indoor Built Environ. 25 (6), 949–961.

Korean Ministry of the Environment (KMOE). Korean Indoor Air Quality Control Act, Amendment No. 15583 (2005).

Korean Ministry of the Environment (KMOE). Strict management of indoor air quality in public transportation such as subways. Press/Explanation. Published April 2, 2020. [accessed September 4, 2021]. http://www.me.go.kr/home/web/board/read.do?menuId=286&boardMasterId=1&boardCategoryId=39&boardId=1362840.

Lee, S., Kim, M.J., Pyo, S.H., Kim, J.T., Yoo, C.K., 2015. Evaluation of an optimal ventilation IAQ control strategy using control performance assessment and energy demand. Energ. Buildings 98, 134–143. https://doi.org/10.1016/j.enbuild.2014.08.040.

Lee, Y., Lee, Y.C., Kim, T., Choi, J.S., Park, D., 2018. Sources and characteristics of particulate matter in subway tunnels in Seoul, Korea. Int. J. Environ. Res. Public Health 15 (11), 2534.

Liu, H., Lee, S., Kim, M., Shi, H., Kim, J.T., Wasewar, K.L., Yoo, C., 2013. Multi-objective optimization of indoor air quality control and energy consumption minimization in a subway ventilation system. Energ. Buildings 66, 553–561.

Loxham, M., Cooper, M.J., Gerlofs-Nijland, M.E., Cassee, F.R., Davies, D.E., Palmer, M.R., Teagle, D.A.H., 2013. Physicochemical characterization of airborne particulate matter at a mainline underground railway station. Environ. Sci. Tech. 47 (8), 3614–3622. https://doi.org/10.1021/es304481m.

Loxham, M., Nieuwenhuijsen, M.J., 2019. Health effects of particulate matter air pollution in underground railway systems – A critical review of the evidence. Part. Fibre Toxicol. 16 (1) https://doi.org/10.1186/s12989-019-0296-2.

Loy-Benitez, J., Li, Q., Ifaei, P., Nam, K., Heo, S., Yoo, C., 2018. A dynamic gain-scheduled ventilation control system for a subway station based on outdoor air quality conditions. Build. Environ. 144, 159–170. https://doi.org/10.1016/j.buildenv.2018.08.016.

Loy-Benitez, J., Li, Q., Nam, K., Nguyen, H.T., Kim, M., Park, D., Yoo, C., 2021. Multi-objective optimization of a time-delay compensated ventilation control system in a subway facility – A harmony search strategy. Build. Environ. 190 https://doi.org/10.1016/j.buildenv.2020.107543.

Lu, S., Liu, D., Zhang, W., Liu, P., Fei, Y., Gu, Y., Wu, M., Yu, S., Yonemochi, S., Wang, X., Wang, Q., 2015. Physico-chemical characterization of PM2.5 in the microenvironment of Shanghai subway. Atmospheric Research, (2015), 543-552, 153.

Luglio, D.G., Katsigeorgis, M., Hess, J., Kim, R., Adragna, J., Raja, A., Gordon, C., Fine, F., Thurston, G., Gordon, T., Vilcassim, M.J.R., 2021. PM2.5 Concentration and composition in subway systems in the Northeastern United States. Environ. Health Perspect. 129 (2), 027001 https://doi.org/10.1289/ehp7202.

Martins, V., Moreno, T., Minguillón, M.C., Amato, F., de Miguel, E., Capdevila, M., Querol, X., 2015. Exposure to airborne particulate matter in the subway system. Sci. Total Environ. 511, 711–722. https://doi.org/10.1016/j.scitotenv.2014.12.013.

Martins, V., Moreno, T., Mendes, L., Eleftheriadis, K., Diapouli, E., Alves, C.A., Duarte, M., de Miguel, E., Capdevila, M., Querol, X., Minguillón, M.C., 2016. Factors controlling air quality in different European subway systems. Environ. Res. 146, 35–46. https://doi.org/10.1016/j.envres.2015.12.007.

Minguillón, M.C., Reche, C., Martins, V., Amato, F., de Miguel, E., Capdevila, M., Centelles, S., Querol, X., Moreno, T., 2018. Aerosol sources in subway environments. Environ. Res. 167, 314–328. https://doi.org/10.1016/j.envres.2018.07.034.

Moreno, T., de Miguel, E., 2018. Improving air quality in subway systems: An overview. Environ. Pollut. 239, 829–831. https://doi.org/10.1016/j.envpol.2018.01.077.

Moreno, T., Pérez, N., Reche, C., Martins, V., de Miguel, E., Capdevila, M., Centelles, S., Minguillón, M.C., Amato, F., Alastuey, A., Querol, X., Gibbons, W., 2014. Subway platform air quality: Assessing the influences of tunnel ventilation, train piston effect and station design. Atmos. Environ. 92, 461–468. https://doi.org/10.1016/j.atmosenv.2014.04.043.

Moreno, T., Martins, V., Querol, X., Jones, T., BéruBé, K., Minguillón, M.C., Amato, F., Capdevila, M., de Miguel, E., Centelles, S., Gibbons, W., 2015. A new look at inhalable metalliferous airborne particles on rail subway platforms. Sci. Total Environ. 505, 367–375. https://doi.org/10.1016/j.scitotenv.2014.10.013.

Moreno, T., Querol, X., Martins, V., Minguillón, M.C., Reche, C., Ku, L.H., Eun, H.R., Ahn, K.H., Capdevila, M., De Miguel, E., 2017a. Formation and alteration of airborne particles in the subway environment. Environ. Sci. Process. Impacts. 19 (1) https://doi.org/10.1039/c6em00576d.

Moreno, T., Reche, C., Minguillón, M.C., Capdevila, M., de Miguel, E., Querol, X., 2017b. The effect of ventilation protocols on airborne particulate matter in subway systems. Sci. Total Environ. 584–585, 1317–1323. https://doi.org/10.1016/j.scitotenv.2017.02.003.

Park, D., Oh, M., Yoon, Y., Park, E., & Lee, K. (2012). Source identification of PM 10 pollution in subway passenger cabins using positive matrix factorization. Atmospheric Environment, 49, 180–185. https://doi.org/10.1016/j.atmosenv.2011.11.064.

Park, D., Lee, T., Hwang, D., Jung, W., Lee, Y., Cho, K., Kim, D., Lee, K., 2014a. Identification of the sources of PM10 in a subway tunnel using positive matrix factorization. J. Air Waste Manag. Assoc. 64 (12), 1361–1368. https://doi.org/10.1080/10962247.2014.950766.

Park, J.H., Woo, H.Y., Park, J., C., 2014b. Major factors affecting the aerosol particulate concentration in the underground stations. Indoor Built Environ. 23 (5), 629–639. https://doi.org/10.1177/1420326X12466875.

Park, J.H., Son, Y.S., Kim, K.H., 2019. A review of traditional and advanced technologies for the removal of particulate matter in subway systems. Indoor Air 29 (2), 177–191. https://doi.org/10.1111/ina.12532.

Querol, X., Moreno, T., Karanasiou, A., Reche, C., Alastuey, A., Viana, M., Font, O., Gil, J., De Miguel, E., Capdevila, M., 2012. Variability of levels and composition of PM10 and PM2.5 in the Barcelona metro system. Atmos. Chem. Phys. 12 (11), 5055–5076. https://doi.org/10.5194/acp-12-5055-2012.

Ravel, B., Newville, M., 2005. ATHENA, ARTEMIS, HEPHAESTUS: data analysis for X-ray absorption spectroscopy using IFEFFIT. J. Synchrotron Radiat. 12 (4), 537–541.

Saunders, B.M., Smith, J.D., Smith, T.E.L., Green, D.C., Barratt, B., 2019. Spatial variability of fine particulate matter pollution (PM2.5) on the London Underground network. Urban Clim. 30, 1–3. https://doi.org/10.1016/j.uclim.2019.100535.

Smith, J.D., Barratt, B.M., Fuller, G.W., Kelly, F.J., Loxham, M., Nicolosi, M., Priestman, M., Tremper, A.H., Green, D.C., 2020. PM2.5 on the London Underground. Environ. Int. 134 https://doi.org/10.1016/j.envint.2019.105188.

State of Washington Department of Ecology (SWDE), 2011. Copper and Zinc Loading Associated with Automotive Brake-Pad and Tire Wear. Publication no. 11-10-087.

Taiwan Indoor Air Quality Management Act (TIAQMA). Promulgated by Presidential Order Hua-Tsung-Yi-Yi-Tzu No. 10000259721 on November 23, 2011.

Toronto Public Health (TPH), 2020. Subway Health Impacts Study. https://www.toronto.ca/legdocs/mmis/2020/hl/bgrd/backgroundfile-141357.pdf.

U.S. Environmental Protection Agency, 2004a. EPA-CMB8.2 Users Manual. Report No. EPA452/R-04-011. December 2004. Office of Air Quality Planning & Standards, Research Triangle Park, NC, www.epa.gov/ttn/SCRAM/receptor_cmb.htm.

US EPA. Risk Assessment Guidance for Superfund , Volume I: Human Health Evaluation Manual (Part 676 F, Supplemental Guidance for Inhalation Risk Assessment) 2009.

[US EPA] United States Environmental Protection Agency (2014). EPA Positive Matrix Factorization (PMF) 5.0 Fundamentals and User Guide. EPA/600/R-14/108, April 2014, US EPA, Washington, DC. https://www.epa.gov/sites/default/files/2015-02/documents/pmf_5.0_user_guide.pdf.

Van Ryswyk, K., Anastasopolos, A., Evans, G., Sun, L., Sabaliauskas, K., Kulka, R., Wallace, L., Weichenthal, S., 2017. Metro Commuter exposures to particulate air pollution and PM2.5-associated elements in Three Canadian Cities: the Urban Transportation Exposure Study. Environ. Sci. Tech. 51 (10), 5713–5720. https://doi.org/10.1021/acs.est.6b05775.

Van Ryswyk, K., Kulka, R., Marro, L., Yang, D., Toma, E., Mehta, L., McNeil-Taboika, L., Evans, G., 2021. Impacts of subway system modification on air quality in subway platforms and trains. Environ. Sci. Tech. 55 (16), 11133–11143. https://doi.org/10.1021/acs.est.1c00703.

Xu, B., Hao, J., 2017. Air quality inside subway metro indoor environment worldwide: a review. Environ. Int. 107, 33–46. https://doi.org/10.1016/j.envint.2017.06.016.

Zhao, L., Wang, J., Gao, H.O., Xie, Y., Jiang, R., Hu, Q., Sun, Y., 2017. Evaluation of particulate matter concentration in Shanghai's metro system and strategy for improvement. Transp. Res. Part D: Transp. Environ. 53, 115–127. https://doi.org/10.1016/j.trd.2017.04.010.